Elite Master Course Theoretical and Mathematical Physics

Master's Thesis

Arrival Time Distributions of Spin-1/2 Particles

Siddhant Das

October 25, 2017

Supervised by Prof. Dr. Detlef Dürr

Arrival time distributions of spin-1/2 particles

Siddhant Das

October 25, 2017

Declaration

I declare that this thesis is an original report of my research, has been written by me and has not been submitted for any previous degree. Due references have been provided on all supporting literature and resources.

Siddhant Das

Acknowledgements

Contents

1   A 'thought' experiment

Consider the following experiment: A spin-1/2 particle is constrained to move within a semi-infinite cylindrical waveguide of radius ρ, with a potential barrier constructed at a distance d from the end face of the waveguide. Initially the barrier is made impenetrable, trapping the particle within a cylindrical box of width d formed between the end face of the waveguide and the barrier. At the start of the experiment the barrier is suddenly switched off, allowing the particle to propagate freely within the waveguide. We ask, *how long* does it take for the particle to arrive at a distance $L > d$ (from the end face of the waveguide) for the first time? In particular, if the experiment is repeated several times, with the particle taking apparently random times to span the same distance L, we ask for the *distribution* of these arrival times.

2   Background and motivation

The prediction of first arrival time of a quantum particle has a long history [1]. The very notion of arrival or tunneling time of a particle is not well posed within the orthodox (or Copenhagen) interpretation of quantum mechanics, since the particle is said to not have a well defined position at a given instant of time. However, the problem of time, or the problem of timing the motion of quantum particles surfaced long before any known interpretations of quantum mechanics came into being. As early as 1925, shortly after the invention of matrix mechanics, Wolfgang Pauli wrote to Niels Bohr:

"In the new theory, all physically observable quantities still do not really occur. Absent, namely, are the time instants of transition processes, which are certainly in principle observable (as for example, are the instants of the emission of photoelectrons). It is now my firm conviction that a really satisfying physical theory must not only involve no unobservable quantities, but must also connect all observable quantities with each other. Also, I remain convinced that the concept of 'probability' should not occur in the fundamental laws of a satisfying physical theory."

Pauli's early views on the problem of time in quantum mechanics deeply influenced the subsequent research on this subject. In particular, he showed that a self-adjoint time operator $\hat{T}$, canonically conjugate to the Hamiltonian $\hat{H}$, viz.

$$[\hat{H}, \hat{T}] = i\hbar \tag{1}$$

implied that the spectrum of $\hat{H}$ would be unbounded from below, which in turn implied that matter couldn't be stable. This result raised doubts on the status of the 'time-energy uncertainty relation'

$$\Delta E \, \Delta T \geq \frac{\hbar}{2}. \tag{2}$$

Despite these impediments, many physicists have attempted to incorporate a respectable time observable by extending the basic framework of quantum theory [4]. These proposals are yet to be checked by experiments.

On the other hand, it has also long been realized that quantum theories comprising of actual particle trajectories, such as Bohmian Mechanics (BM) [2] and Nelson's stochastic mechanics [3] provide a natural framework for addressing this problem. In such theories, when the particle moves on a trajectory $\boldsymbol{R}(t, \boldsymbol{R}_0)$, where $\boldsymbol{R}_0$ is the initial position of the particle lying in the support of the (compactly supported) initial wave function ψ_0, the time of first arrival on a

surface Σ placed outside the support of ψ_0 is given by

$$\tau(\boldsymbol{R}_0) = \inf\{t \,|\, \boldsymbol{R}(t, \boldsymbol{R}_0) \in \Sigma, \, \boldsymbol{R}_0 \in \mathrm{supp}(\psi_0)\}. \tag{3}$$

Since the initial position $\boldsymbol{R}_0$ is always assumed to be $|\psi_0|^2$-distributed (Born's statistical law), the time of first arrival is random as is the position where the particle crosses Σ. While the distribution of $\tau(\boldsymbol{R}_0)$ will in general be only numerically accessible, it has been conjectured–at least in the case of Bohmian Mechanics–that it provides a good prediction for the statistics in a measurement of first arrival times. Such measurements have unfortunately not been performed until now. The conjecture has however to be taken cum grano salis as we shall explain. First note that the definition (3) applies to all versions of quantum mechanics in which particles move on trajectories. As remarked before, there are many such versions apart from Bohmian Mechanics; for example in Nelson's stochastic mechanics, the particle exhibits Brownian like motion. In view of this it is clear that the distributions of first arrival times will differ considerably for the different versions, but the theories are nevertheless *empirically equivalent*. To understand this it is good to recall the following theorem [5]:

"*All measured quantum statistics are given by positive operator valued measures (POVMs) on a Hilbert space.*"

This means that for a given experimental setup for measuring first arrival times, there will be a POVM associated with that experiment on the Hilbert space of the particle which determines for any initial wave function of the particle the statistics of the readings of the apparatus[1].

Empirically equivalent versions of quantum mechanics would, when the experiment were theoretically analyzed, predict that POVM. However, the theoretical analysis could be rather different in the different versions, for example it may be the case that $\tau(\boldsymbol{R}_0)$ itself plays little or no role. This is because the determination of the POVM associated with the given experiment will in general depend on the full quantum mechanical analysis of the combined system of apparatus and particle, i.e. on solving Schrödinger's equation for the entangled wave function of the combined system. Since this is practically impossible, there have been many attempts to guess a universal POVM or a universal class of POVMs from symmetry or other principles of orthodox quantum mechanics, which should be close to the true POVM of a given experiment, where closeness means that the statistics of the universal POVMs are close to the registered statistics [4, 8] of the hopefully sometimes soon to be performed arrival time experiment. So far none of the POVMs have been experimentally verified in a serious manner.

Focusing now on Bohmian Mechanics we see that the guidance law for the particle's motion (given in Eq. (7) below) is nonlinear in the wave function, with the nonlinearity being such that it is inconceivable that the distribution of $\tau(\boldsymbol{R}_0)$ is given by a POVM, which must be bilinear in ψ_0. But in the so called scattering regime, i.e. when the surface Σ is far from the support of ψ_0 it has been shown that the probability distribution of $\tau(\boldsymbol{R}_0)$ is given by

$$\varrho^{\psi_0}(t < \tau \leq t + \mathrm{d}t) = \int_\Sigma \boldsymbol{j}^{\psi_t} \cdot \mathrm{d}\boldsymbol{\Sigma}\, \mathrm{d}t \tag{4}$$

where

$$\boldsymbol{j}^{\psi_t} = \frac{\hbar}{m} \mathrm{Im}[\psi_t^* \boldsymbol{\nabla} \psi_t] \tag{5}$$

---

[1]The theorem does not apply to generalized notions of measurements like e.g. *weak measurements*. In the latter the weakly measured values are averages conditioned on a selected sub-ensemble. The selection of sub-ensembles makes such "measurements" nonlinear [6] in contrast to the standard measurements, which are in that sense linear and to which the theorem applies.

is the probability current density defined in terms of the particle's wave function ψ_t. It satisfies the continuity equation

$$\frac{\partial}{\partial t}|\psi_t|^2 + \boldsymbol{\nabla} \cdot \boldsymbol{j}^{\psi_t} = 0. \tag{6}$$

The probability $\boldsymbol{j}^{\psi_t} \cdot \mathrm{d}\boldsymbol{\Sigma} \, \mathrm{d}t$ leads directly to the quantum mechanical $S-$matrix formalism, which is experimentally verified. In this asymptotic sense the flux defines a POVM and in this asymptotic sense the first arrival distribution defines a POVM.

The connection between the left and the right hand side of (4) is based on the fact that the current density $\boldsymbol{j}^{\psi_t}$ actually defines the Bohmian guiding law for spinless particles: The trajectory $\boldsymbol{R}(t)$ of the particle is governed by the differential equation

$$\dot{\boldsymbol{R}}(t) = \frac{\boldsymbol{j}^{\psi_t}(\boldsymbol{R}(t))}{|\psi_t|^2(\boldsymbol{R}(t))}\,. \tag{7}$$

In view of other trajectory based versions of quantum mechanics, we remark that formula (4) does not hold, for instance in Nelson's stochastic mechanics.

When the surface Σ is near to the support of the initial wave function, equation (4) is no longer true, since the right hand side can become negative, which implies that the quantum flux lines, or the Bohmian trajectories cross the surface Σ several times by crossing back and forth through the surface, while in the scattering regime the trajectories become straight lines and they cross only once. Since in the scattering regime, the probability distribution for first arrival times of the Bohmian trajectories is experimentally verified in scattering experiments, it is natural to conjecture that the Bohmian first arrival time distribution, which can be computed numerically will still be close to the measured distribution, for non pathological wave functions. By non pathological wave functions we mean wave functions which can be prepared, e.g. ground states in a trap. As we stressed above, it cannot reproduce the first arrival time distributions for all wave functions, since it is in general not a POVM.

There is however a caveat one needs to take note of. Measurement is an interaction that always affects the wave function in terms of back scattering. This effect changes the Bohmian trajectories guided by the wave function and hence changes the arrival time distribution determined by the unperturbed wave function. For simplicity we ignore this effect in our discussion. In this thesis, we will be concerned with what are known as *intrinsic* or *ideal* arrival time distributions without referring to a particular measurement procedure. In § 9 we discuss experimental questions like initial state preparation, measurement etc. at length.

The relevant ingredients of Bohmian mechanics needed for an analysis of our experiment are presented in the next section. We also compare the Bohmian arrival time statistics with the so-called semiclassical formula, which is determined from the momentum distribution of the particle. This formula tends to agree with other approaches in the scattering regime, but is highly doubtful to be correct in the near field regime.

3 Elements of Bohmian mechanics

In the de Broglie-Bohm pilot wave theory, or Bohmian mechanics, a spin-1/2 particle is a point particle, whose sole attribute is a *position* in space at time t, denoted by $\boldsymbol{R}(t) \in \mathbb{R}^3$. In the course of time, the particle moves on a deterministic (Bohmian) *trajectory* $\boldsymbol{R}$ with velocity vector $\dot{\boldsymbol{R}}$ specified by the *guidance law* [12, 13]

$$\dot{\boldsymbol{R}}(t) = \frac{\hbar}{m}\mathrm{Im}\left[\frac{\Psi^\dagger\boldsymbol{\nabla}\Psi}{\Psi^\dagger\Psi}\right](\boldsymbol{R}(t),t) + \frac{\hbar}{2m}\left[\frac{\boldsymbol{\nabla}\times(\Psi^\dagger\boldsymbol{\sigma}\Psi)}{\Psi^\dagger\Psi}\right](\boldsymbol{R}(t),t)\,. \tag{8}$$

Here,

$$\Psi(\boldsymbol{r}, t) = \begin{pmatrix} \psi_+(\boldsymbol{r}, t) \\ \psi_-(\boldsymbol{r}, t) \end{pmatrix} \tag{9}$$

is a complex-valued spinor wave function, satisfying the Pauli wave equation

$$i\hbar\frac{\partial}{\partial t}\Psi(\boldsymbol{r}, t) = -\frac{\hbar^2}{2m}\left(\boldsymbol{\sigma}\cdot\boldsymbol{\nabla}\right)^2\Psi(\boldsymbol{r}, t) + V(\boldsymbol{r}, t)\Psi(\boldsymbol{r}, t), \tag{10}$$

where $V(\boldsymbol{r}, t)$ is an external potential characterizing the interactions of the particle with its surroundings, while

$$\boldsymbol{\sigma} := \sigma_x\,\hat{\boldsymbol{x}} + \sigma_y\,\hat{\boldsymbol{y}} + \sigma_z\,\hat{\boldsymbol{z}} \tag{11}$$

is a 3-vector of Pauli matrices. Note that the vector $\boldsymbol{r}$ in the argument of Ψ is a mere place holder, and shouldn't be confused with an actual particle position $\boldsymbol{R}(t)$. One may regard the wave function Ψ as a convenient parameterization of the particle velocity in space-time.

Since $\boldsymbol{R}(t)$ doesn't appear in the wave equation, it can be solved autonomously, given an initial condition $\Psi(\boldsymbol{r}, 0)$. Similarly, knowledge of the initial particle position $\boldsymbol{R}(0)$ on a trajectory suffices to solve equation (8). However, if the trajectory encounters a zero (or node) of the wave function it cannot be continued further, since the velocity $\dot{\boldsymbol{R}}$ becomes unbounded there. Luckily, general theorems guaranteeing the global existence of Bohmian trajectories exist, which show that the singularities of the velocity field will not be reached in finite time for typical initial conditions [14, 15].

Applying these equations to any physical situation of interest, one achieves a vivid description of quantum mechanical processes, which is lacking in the operational approaches to quantum mechanics. See [16, 17, 18, 19] for an analysis of the Stern-Gerlach experiment and neutron interferometry. The Bohmian analysis of the double-slit experiment with spin-1/2 particles is given in [13].

Equations (8–10) apply to a single spin-1/2 particle placed in an external potential field V, and can be generalized to account for many interacting particles [20]. Thus using the many-body guidance law, one can study the motion of electrons in simple atoms like hydrogen [21, 22] and helium [23]. Radiative transitions in hydrogen atoms driven by an external electromagnetic field are discussed in [24, 25], while the non-local spin correlations of the EPR-B experiment have been explained in [17, 26] using the guidance law.

4   Formulation

In this section we present a detailed analysis of the experiment outlined in Section 1 using the dynamical equations of Bohmian mechanics. Let the cylindrical waveguide be mounted on the $xy-$plane of a right-handed coordinate system, the axis of the cylinder defining the $z-$axis, and let the barrier at $z = d$ be switched off at $t = 0$.

Employing cylindrical coordinates $(\imath, \phi, z)$, the potential field of the waveguide may be written as

$$V(\boldsymbol{r}) = V_\perp(\imath) + V_\parallel(z) \tag{12}$$

for $t > 0$. Here,

$$V_\perp(\imath) = \frac{1}{2}m\omega^2\imath^2 \tag{13}$$

is a transverse confining potential, and

$$V_\parallel(z) = \begin{cases} \infty & z \leq 0 \\ 0 & z > 0 \end{cases} \tag{14}$$

is the axial potential, comprised of an impenetrable hard wall at $z = 0$, which defines the end face of the waveguide. The choice of a harmonic confinement in the transverse direction is motivated in part by mathematical simplicity, but more importantly by experimental considerations. For instance, the radial potential profile encountered by electrons propagating in semiconductor waveguides is well approximated by the harmonic potential [27]. These structures have typical radii $\rho \approx 0.5\,\mu m$ and trap widths $d \approx 5\,nm$. Single neutrons stored in Penning traps also experience harmonic confinements, remaining stable (to beta decay) for about $870\,s$ [28].

Beside fundamental particles, composite species like calcium $^{40}_{20}Ca^+$, ytterbium $^{171}_{70}Yb^+$ and barium $^{137}_{56}Ba^+$ ions featuring an unpaired electron, behave like spin-1/2 particles. These ions can be easily isolated and trapped in radio frequency linear Paul traps, which provide harmonic confinements up to radial distances $\rho \approx 1\,mm$, with a characteristic $\omega \approx 5 - 100\,MHz$ [29]. An optical barrier may be added to this assembly at a distance $d \approx 10\,\mu m$ from one of the end-caps, where the distance between the end-caps defines the length of the waveguide ($\approx 6\,mm$).

The wave functions in a harmonic potential have Gaussian tails, characterized by a length scale of $\sqrt{\hbar/m\omega}$, which for a calcium ion of mass $m \approx 5.18 \times 10^{-26}\,kg$ and trapping frequency $\omega \approx 50\,MHz$ equals $\approx 6.4 \times 10^{-9}\,m$. Since the waveguide radius ρ is much larger than this (decay) length, it can be set to ∞ for practical calculations. From here on, we will also set $\hbar = m = d = 1$ in all equations for convenience. These constants may be restored with the substitutions

$$a \to \frac{a}{d}, \qquad \Psi \to d^{-3/2}\Psi, \qquad \omega \to \frac{md^2}{\hbar}\omega, \qquad t \to \frac{\hbar}{md^2}t, \tag{15}$$

where $a = \imath, z, L, \boldsymbol{R}$.

We will further assume that the particle was prepared in one of the ground states of the trap at the instant when the potential barrier was turned off.[2] Since the ground state of the cylindrical box for a spin-1/2 particle is doubly degenerate, any ground state wave function can be conveniently parameterized with two real parameters (see appendix A). The wave function of the particle at $t = 0$, thus has the general form

$$\Psi(\boldsymbol{r}, 0) = \psi_0(\boldsymbol{r}) \begin{pmatrix} \cos(\alpha/2) \\ \sin(\alpha/2)\,e^{i\beta} \end{pmatrix}, \tag{16}$$

where

$$0 \leq \alpha \leq \pi, \quad 0 \leq \beta < 2\pi$$

characterize the 'spin part' of the wave function,

$$\psi_0(\boldsymbol{r}) = \sqrt{\frac{2\omega}{\pi}}\,\theta(z)\theta(1 - z)\sin(\pi z)\exp\left(-\frac{\omega}{2}\imath^2\right) \tag{17}$$

is the 'spatial part' of the wave function, and $\theta(x)$ is the Heaviside step function.

4.1 Time evolution of wave function

We begin by solving the time dependent Pauli equation:

$$i\frac{\partial}{\partial t}\Psi(\boldsymbol{r}, t) = -\frac{1}{2}\nabla^2\Psi(\boldsymbol{r}, t) + \frac{1}{2}\omega^2\imath^2\Psi(\boldsymbol{r}, t) + V_\parallel(z)\Psi(\boldsymbol{r}, t), \tag{18}$$

---

[2]We discuss state preparation in a later section.

with initial condition (16). In writing equation (18) we have used the identity

$$(\boldsymbol{\sigma}\cdot\boldsymbol{\nabla})^2 = \nabla^2\mathbb{1} \tag{19}$$

(denoting the 2×2 unit matrix by $\mathbb{1}$), which follows readily from the algebraic properties of the Pauli matrices, viz.

$$\begin{aligned}
(\boldsymbol{\sigma}\cdot\boldsymbol{\nabla})^2 &= \sum_{a,b=1}^{3} \sigma_a\partial_a\sigma_b\partial_b = \sum_{a,b=1}^{3} \partial_a\partial_b\sigma_a\sigma_b \\
&= \sum_{a,b=1}^{3} \delta_{ab}\,\partial_a\partial_b\mathbb{1} + i\sum_{a,b,c=1}^{3} \varepsilon_{abc}\,\partial_a\partial_b\sigma_c \\
&= \nabla^2\mathbb{1}.
\end{aligned}$$

Considering the form of the initial wave function, we make the ansatz

$$\Psi(\boldsymbol{r},t) = \psi(\boldsymbol{r},t)\begin{pmatrix} \cos(\alpha/2) \\ \sin(\alpha/2)\,e^{i\beta} \end{pmatrix} \tag{20}$$

for the time dependent wave function. It satisfies equation (18), iff $\psi(\boldsymbol{r},t)$ solves the Schrödinger equation

$$i\frac{\partial}{\partial t}\psi(\boldsymbol{r},t) = \hat{H}\psi(\boldsymbol{r},t), \tag{21}$$

where

$$\hat{H} := -\frac{1}{2}\nabla^2 + \frac{1}{2}\omega^2\varrho^2 + V_\|(z). \tag{22}$$

Further, letting

$$\psi(\boldsymbol{r},0) = \psi_0(\boldsymbol{r}) \tag{23}$$

ensures that equation (16) is satisfied as well.

The solution of the Schrödinger equation can be formally written as

$$\psi(\boldsymbol{r},t) = e^{-it\hat{H}}\psi_0(\boldsymbol{r}), \tag{24}$$

using the unitary time evolution operator $\exp(-it\hat{H})$. This formal solution may be developed further by resolving $\psi_0(\boldsymbol{r})$ in a basis of eigenfunctions of $\hat{H}$. These functions satisfy the usual time independent Schrödinger equation

$$\hat{H}\varphi(\boldsymbol{r}) = E\varphi(\boldsymbol{r}). \tag{25}$$

The eigenfunctions suitable for our purpose may be written as

$$\varphi(\boldsymbol{r}) = \zeta(z)\exp\left(-\frac{\omega}{2}\varrho^2\right). \tag{26}$$

Substituting this ansatz into equation (25), we arrive at an ODE for $\zeta(z)$, viz.

$$-\frac{\mathrm{d}^2}{\mathrm{d}z^2}\zeta(z) + 2V_\|(z)\zeta(z) = k^2\zeta(z), \tag{27}$$

where

$$E = \omega + \frac{k^2}{2}. \tag{28}$$

10

The general solution of equation (27) has the form

$$\zeta(z) = A\,\theta(z)\sin(kz), \quad k > 0 \tag{29}$$

where A is an arbitrary constant.[3] Thus,

$$\varphi_k(\boldsymbol{r}) = A\,\theta(z)\sin(kz)\exp\left(-\frac{\omega}{2}\imath^2\right). \tag{30}$$

Customarily, A is suitably chosen to ensure

$$\int_{\mathbb{R}^3} \mathrm{d}^3\boldsymbol{r}\ \varphi_k(\boldsymbol{r})\varphi_{k'}(\boldsymbol{r}) = \delta(k - k'). \tag{31}$$

This yields

$$A = \frac{\sqrt{2\omega}}{\pi}. \tag{32}$$

Now, expanding the initial wave function as

$$\psi_0(\boldsymbol{r}) = \int_0^\infty \mathrm{d}k\ c(k)\varphi_k(\boldsymbol{r}), \tag{33}$$

we have (by virtue of equation (31))

$$c(k) = \int_{\mathbb{R}^3} \mathrm{d}^3\boldsymbol{r}\ \varphi_k(\boldsymbol{r})\psi_0(\boldsymbol{r}) = 2\sqrt{\pi}\frac{\sin k}{\pi^2 - k^2}. \tag{34}$$

Substituting equation (33), together with equation (28) for the energy eigenvalues, into our formal solution, equation (24), yields

$$\psi(\boldsymbol{r}, t) = \int_0^\infty \mathrm{d}k\ c(k)e^{-it\hat{H}}\varphi_k(\boldsymbol{r}) = \int_0^\infty \mathrm{d}k\ c(k)\,e^{-i\omega t - i\frac{k^2}{2}t}\varphi_k(\boldsymbol{r}). \tag{35}$$

Writing out $\varphi_k(\boldsymbol{r})$, and substituting $c(k)$ from equation (34), we obtain an explicit integral representation of the time dependent wave function

$$\psi(\boldsymbol{r}, t) = 2\sqrt{\frac{2\omega}{\pi}}\theta(z)\exp\left(-\frac{\omega}{2}\imath^2 - i\omega t\right)\int_0^\infty \mathrm{d}k\ \frac{\sin k\sin(kz)}{\pi^2 - k^2}\,e^{-i\frac{k^2}{2}t} \tag{36}$$

For later convenience, we define the 'time evolution integral'

$$W(z, t) \coloneqq \theta(z)\int_{-\infty}^\infty \mathrm{d}k\ \frac{\sin k\sin(kz)}{\pi^2 - k^2}\,e^{-i\frac{k^2}{2}t}, \tag{37}$$

which allows writing the wave function as[4]

$$\psi(\boldsymbol{r}, t) = \sqrt{\frac{2\omega}{\pi}}\exp\left(-\frac{\omega}{2}\imath^2 - i\omega t\right)W(z, t). \tag{38}$$

Fortunately, the time evolution integral can be evaluated in closed form (see appendix B):

$$W(z, t) = \theta(z)\left[\mathscr{D}(z - 1, t) + \mathscr{D}(1 - z, t) - \mathscr{D}(1 + z, t) - \mathscr{D}(-1 - z, t)\right] \tag{39}$$

---

[3]Since $\sin(kz) = -\sin(-kz)$, we will fix $k > 0$ in order that the eigenfunctions are linearly independent.
[4]Exploiting the symmetry of the integrand, the integral has been extended to $-\infty < k < \infty$.

where

$$\mathscr{D}(\xi, t) := \frac{e^{-i\frac{\pi^2}{2}t}}{8i} \left\{ e^{i\pi\xi} \operatorname{erfc}\left[\frac{i^{3/2}}{\sqrt{2}}\left(\frac{\xi}{\sqrt{t}} - \pi\sqrt{t}\right)\right] - e^{-i\pi\xi} \operatorname{erfc}\left[\frac{i^{3/2}}{\sqrt{2}}\left(\frac{\xi}{\sqrt{t}} + \pi\sqrt{t}\right)\right] \right\}, \tag{40}$$

and $\operatorname{erfc}(x)$ is the complementary error function. In the limit $t \to 0^+$

$$W(z, t) \to \theta(z)\theta(1 - z)\sin(\pi z), \tag{41}$$

as a result of the identity[5]

$$\lim_{t\to 0^+} \operatorname{erfc}\left[\frac{i^{3/2}}{\sqrt{2}}\left(\frac{\xi}{\sqrt{t}} \pm \pi\sqrt{t}\right)\right] = 2\,\theta(\xi). \tag{42}$$

This ensures that $\psi(\boldsymbol{r}, t)$ satisfies equation (23). A few snapshots of the time evolution integral are shown in Fig. 1.
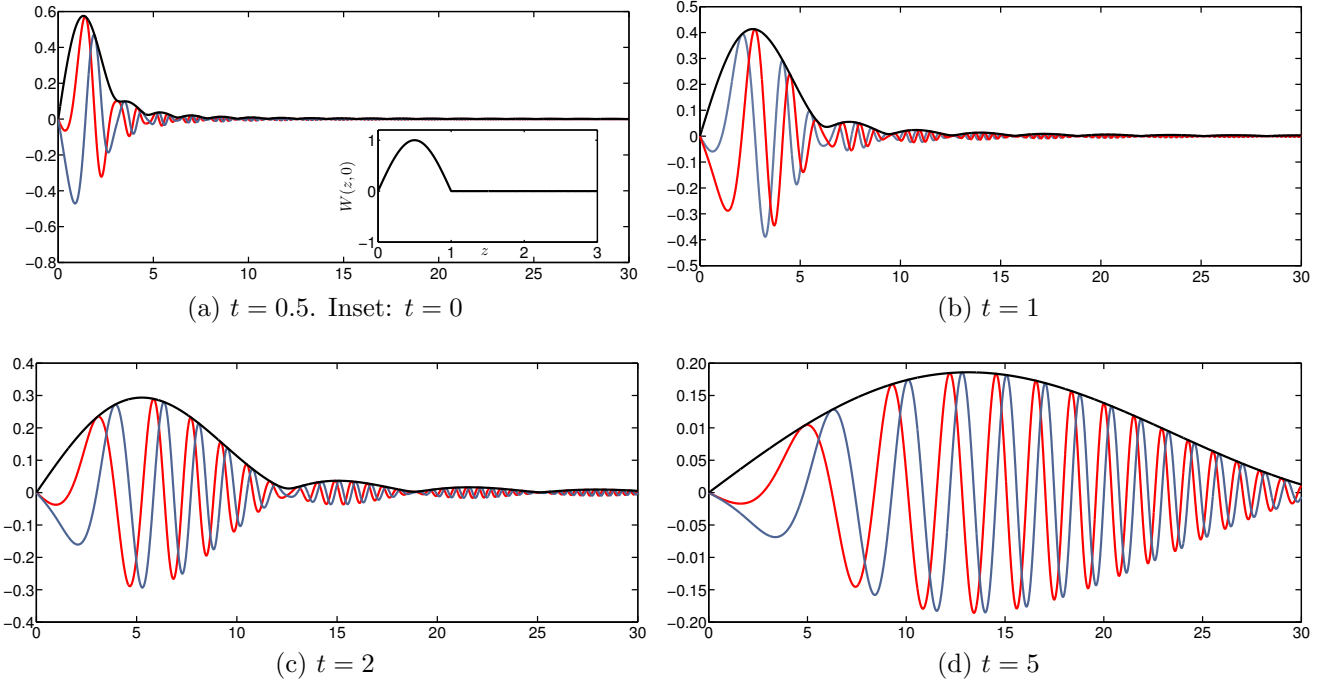

(a) $t = 0.5$. Inset: $t = 0$

(b) $t = 1$

(c) $t = 2$

(d) $t = 5$

Figure 1: Re[W] (red), Im[W] (blue) and |W| (black) vs. z at different instants of time.

4.2 Bohmian trajectories

The particle trajectories are the integral curves of the Bohmian velocity field given in equation (8). It is comprised of the *convective velocity*

$$\boldsymbol{v}_c = \operatorname{Im}\left[\frac{\Psi^\dagger \boldsymbol{\nabla}\Psi}{\Psi^\dagger \Psi}\right] = \operatorname{Im}\left[\frac{\boldsymbol{\nabla}\psi}{\psi}\right] = \operatorname{Im}\left[\frac{W'}{W}\right]\hat{\boldsymbol{z}}, \tag{43}$$

where $W' = \partial W/\partial z$, and the *spin velocity*

$$\boldsymbol{v}_s = \frac{1}{2}\left[\frac{\boldsymbol{\nabla}\times(\Psi^\dagger \boldsymbol{\sigma}\Psi)}{\Psi^\dagger \Psi}\right] = \left[\frac{\boldsymbol{\nabla}\times(|\psi|^2\boldsymbol{s})}{|\psi|^2}\right]. \tag{44}$$

---

[5]See identity (19) of [30].

12
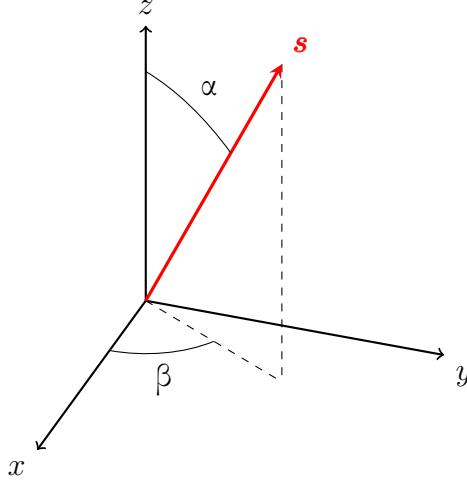
Figure 2: Spin vector $\boldsymbol{s}$

Here,

$$\boldsymbol{s} = \frac{1}{2}\big(\sin\alpha\,\cos\beta\,\hat{\boldsymbol{x}} + \sin\alpha\,\sin\beta\,\hat{\boldsymbol{y}} + \cos\alpha\,\hat{\boldsymbol{z}}\big) \tag{45}$$

is the *spin vector* depicted in Fig. 2. Resolving the Cartesian unit vectors along the unit vectors in cylindrical coordinates, viz.

$$\hat{\boldsymbol{x}} = \cos\phi\,\hat{\boldsymbol{\imath}} - \sin\phi\,\hat{\boldsymbol{\phi}} \tag{46a}$$

$$\hat{\boldsymbol{y}} = \sin\phi\,\hat{\boldsymbol{\imath}} + \cos\phi\,\hat{\boldsymbol{\phi}} \tag{46b}$$

we can transform the spin vector $\boldsymbol{s}$ to it's cylindrical equivalent, viz.

$$\boldsymbol{s} = \frac{1}{2}\big(\sin\alpha\,\cos(\phi-\beta)\,\hat{\boldsymbol{\imath}} - \sin\alpha\,\sin(\phi-\beta)\,\hat{\boldsymbol{\phi}} + \cos\alpha\,\hat{\boldsymbol{z}}\big). \tag{47}$$

This allows one to evaluate $\boldsymbol{\nabla}\times(|\psi|^2\boldsymbol{s})$ conveniently, using the formula for the curl of a vector field in cylindrical coordinates, leading to

$$\boldsymbol{\nabla}\times(|\psi|^2\boldsymbol{s}) = \frac{1}{2}\sin\alpha\,\sin(\phi-\beta)\frac{\partial|\psi|^2}{\partial z}\,\hat{\boldsymbol{\imath}} + \frac{1}{2}\left\{\sin\alpha\,\cos(\phi-\beta)\frac{\partial|\psi|^2}{\partial z} - \cos\alpha\frac{\partial|\psi|^2}{\partial\imath}\right\}\hat{\boldsymbol{\phi}}$$
$$- \frac{1}{2}\sin\alpha\,\sin(\phi-\beta)\frac{\partial|\psi|^2}{\partial\imath}\,\hat{\boldsymbol{z}}. \tag{48}$$

Now, writing $|\psi|^2 = \frac{2\omega}{\pi}\exp(-\omega\imath^2)|W|^2$ from equation (38), the required partial derivatives can be evaluated easily, following which the spin velocity would take the form

$$\boldsymbol{v}_s = \sin\alpha\,\sin(\phi-\beta)\,\mathrm{Re}\left[\frac{W'}{W}\right]\hat{\boldsymbol{\imath}} + \left\{\sin\alpha\,\cos(\phi-\beta)\,\mathrm{Re}\left[\frac{W'}{W}\right] + \omega\imath\cos\alpha\right\}\hat{\boldsymbol{\phi}}$$
$$+ \omega\imath\sin\alpha\,\sin(\phi-\beta)\,\hat{\boldsymbol{z}}. \tag{49}$$

The particle position at time t is

$$\boldsymbol{R}(t) = R(t)\,[\cos\Phi(t)\,\hat{\boldsymbol{x}} + \sin\Phi(t)\,\hat{\boldsymbol{y}}] + Z(t)\,\hat{\boldsymbol{z}}, \tag{50}$$

the time derivative of which is

$$\dot{\boldsymbol{R}}(t) = \dot{R}(t)\,\hat{\boldsymbol{\imath}}(t) + R(t)\,\dot{\Phi}(t)\,\hat{\boldsymbol{\phi}}(t) + Z(t)\,\hat{\boldsymbol{z}}, \tag{51}$$

13

where $\hat{\boldsymbol{\imath}}(t) = \cos\Phi(t)\,\hat{\boldsymbol{x}} + \sin\Phi(t)\,\hat{\boldsymbol{y}}$ and $\hat{\boldsymbol{\phi}}(t) = -\sin\Phi(t)\,\hat{\boldsymbol{x}} + \cos\Phi(t)\,\hat{\boldsymbol{y}}$. The r.h.s of the guidance law, equation (8), can be evaluated using equations (43) and (49), and comparison with the above derivative yields the component equations

$$\dot{R}(t) = \sin\alpha\,\sin(\Phi(t) - \beta)\,\mathrm{Re}\left[\frac{W'}{W}\right](Z(t), t), \tag{52a}$$

$$\dot{\Phi}(t) = \frac{\sin\alpha}{R(t)}\cos(\Phi(t) - \beta)\,\mathrm{Re}\left[\frac{W'}{W}\right](Z(t), t) + \omega\cos\alpha, \tag{52b}$$

$$\dot{Z}(t) = \mathrm{Im}\left[\frac{W'}{W}\right](Z(t), t) + \omega\sin\alpha\,\sin(\Phi(t) - \beta)R(t). \tag{52c}$$

5   Solving equations (52)

We have arrived at a coupled system of non-linear ODEs describing the motion of the spin-1/2 particle. These equations are explicitly time dependent (nonautonomous), which are almost never analytically solvable. As a result, we must resort to numerical methods to gain insight into the dynamics. However, for some special spin orientations[6] we can integrate out one or more position coordinates, thereby decoupling the equations of motion partially or completely.

5.1   Special cases

In this section we consider two special wave functions, viz.

$$\Psi_\uparrow(\boldsymbol{r}, t) = \psi(\boldsymbol{r}, t)\begin{pmatrix} 1 \\ 0 \end{pmatrix}, \tag{53a}$$

$$\Psi_\updownarrow(\boldsymbol{r}, t) = \frac{\psi(\boldsymbol{r}, t)}{\sqrt{2}}\begin{pmatrix} 1 \\ 1 \end{pmatrix}, \tag{53b}$$

which correspond to $\alpha = 0$ and $\alpha = \frac{\pi}{2}$ respectively. We shall refer to $\Psi_\uparrow$ as the *spin-up* wave function, and to $\Psi_\updownarrow$ as the *up-down* wave function.

For the spin-up wave function, the equations of motion simplify greatly, viz.

$$\dot{R}(t) = 0, \tag{54a}$$

$$\dot{\Phi}(t) = \omega, \tag{54b}$$

$$\dot{Z}(t) = \mathrm{Im}\left[\frac{W'}{W}\right](Z(t), t). \tag{54c}$$

Equation (54a) implies that the radial coordinate of the particle remains constant in time

$$R(t) = R(0), \tag{55}$$

hence the Bohmian trajectory lies on a right circular cylinder of radius $R(0)$. Subsequently, integrating equation (54b) yields

$$\Phi(t) = \Phi(0) + \omega t, \tag{56}$$

which implies that the angular velocity of the particle about the $z-$axis is a simple linear function of time, independent of the radial or axial distance. Equation (54c) cannot be integrated analytically, hence we have plotted a few numerical solutions in Fig. 3 as illustrative examples. Here, the trajectories have been integrated from $t = 0$ to $t = 5$.
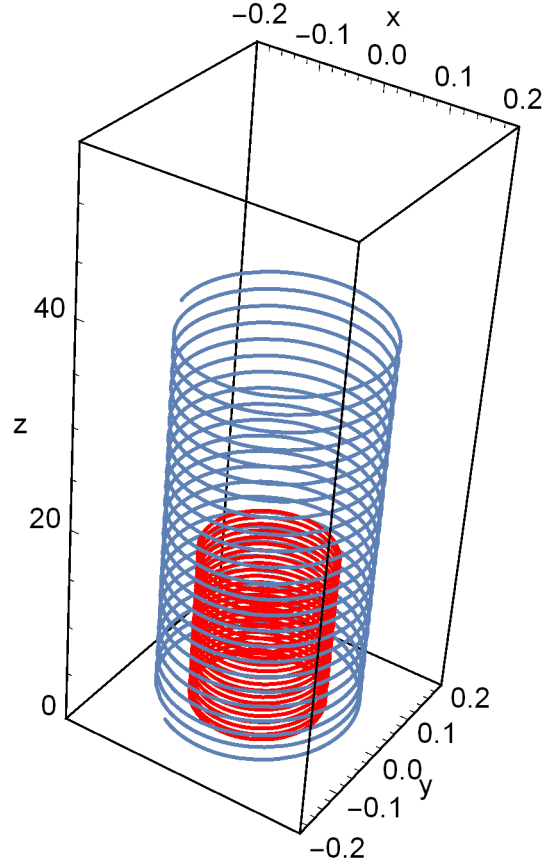
---

[6]Spin orientation refers to a particular α.

Figure 3: Bohmian trajectories for spin-up wave function ($\alpha = 0$) for trapping frequency $\omega = 30$ and initial positions $\boldsymbol{R}(0) = (0.1, \frac{\pi}{6}, 0.6)$ (red), $\boldsymbol{R}(0) = (0.15, \frac{4\pi}{3}, 0.9)$ (blue).

Also Note that a spin-down wave function ($\alpha = \pi$) yields the same equations of motion as above, except for a minus sign on the r.h.s of equation (54b), as a result spin-up and spin-down trajectories arising from the same initial point cover the same axial distance in a given amount of time, but spiral in counterclockwise and clockwise directions respectively.

Now, for the up-down wave function ($\alpha = \pi/2$), the equations of motion take the form

$$\dot{R}(t) = \sin(\Phi(t) - \beta) \operatorname{Re}\left[\frac{W'}{W}\right](Z(t), t), \tag{57a}$$

$$\dot{\Phi}(t) = R^{-1}(t) \cos(\Phi(t) - \beta) \operatorname{Re}\left[\frac{W'}{W}\right](Z(t), t), \tag{57b}$$

$$\dot{Z}(t) = \operatorname{Im}\left[\frac{W'}{W}\right](Z(t), t) + \omega R(t) \sin(\Phi(t) - \beta). \tag{57c}$$

Dividing equation (57a) by equation (57b), we obtain

$$\frac{\mathrm{d}}{\mathrm{d}t} \ln R(t) = \tan(\Phi(t) - \beta) \frac{\mathrm{d}\Phi}{\mathrm{d}t} = -\frac{\mathrm{d}}{\mathrm{d}t} \ln |\cos(\Phi(t) - \beta)|, \tag{58}$$

which upon integration yields an *integral of motion*

$$R(t) |\cos(\Phi(t) - \beta)| = \text{const.} \tag{59}$$

Since this equation holds at all times on the trajectory, one can fix the constant of integration

15

from the initial conditions, obtaining

$$\frac{R(t)}{R(0)} = \left| \frac{\cos(\Phi(0) - \beta)}{\cos(\Phi(t) - \beta)} \right|. \tag{60}$$

We can also rewrite equation (59) in terms of the $xy-$coordinates of the particle, as

$$|\cos\beta\, X(t) + \sin\beta\, Y(t)| = \text{const.}$$
$$\Rightarrow Y(t) = -\cot\beta\, X(t) \pm \frac{\text{const.}}{\sin\beta} \tag{61}$$

This implies that the $xy-$projection of the particle trajectory lies on a straight line, which is inclined at an angle $\frac{\pi}{2} + \beta$ to the $x-$axis. Figure 4 plots a few Bohmian trajectories for the up-down wave function, which were integrated from $t = 0$ to $t = 20$.
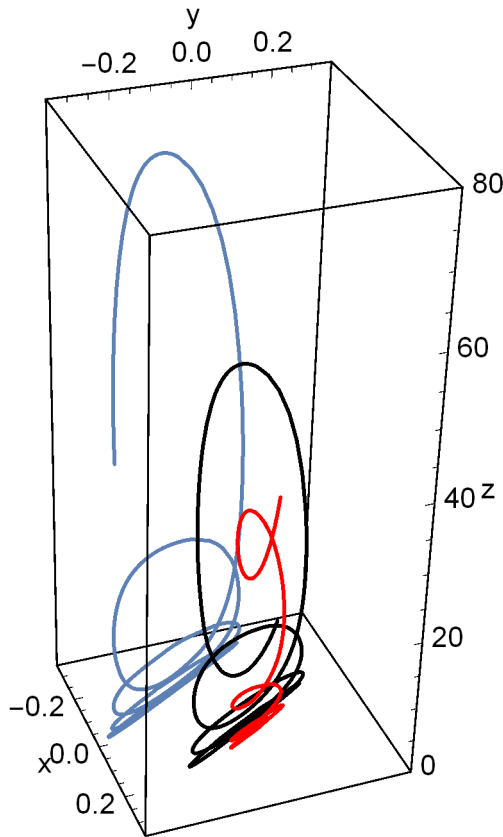

Figure 4: Bohmian trajectories for up-down wave function ($\alpha = \frac{\pi}{2}$) for trapping frequency $\omega = 50$, $\beta = \frac{\pi}{6}$ and initial positions $\boldsymbol{R}(0) = (0.1, \frac{\pi}{3}, 0.6)$ (red), $\boldsymbol{R}(0) = (0.2, \frac{4\pi}{3}, 0.9)$ (blue), $\boldsymbol{R}(0) = (0.06, \frac{\pi}{6}, 0.1)$ (black). Note that the $xy-$projections of the trajectories are straight lines, inclined at an angle $\frac{2\pi}{3}$ $\left(= \frac{\pi}{2} + \beta\right)$ to the $x-$axis.

5.2 General spin orientations

For general spin orientations the equations of motion (52) become analytically intractable, hence we cannot comment on the universal features of the solutions as before. In these circumstances, one could, for instance apply techniques of asymptotic analysis for understanding the long time behavior of the trajectories, or develop various perturbative expansions about the special cases

considered above. Even strong confinement conditions (i.e. large ω) can allow for interesting perturbative calculations. We will not pursue these directions here, as they are not relevant for the discussion of first arrival time statistics. In Fig 5 we plot a few numerically generated Bohmian trajectories for $\alpha = \frac{3\pi}{5}$ and two different trapping frequencies $\omega = 30$ and $\omega = 60$. All trajectories have been integrated from $t = 0$ to $t = 5$ in these examples.
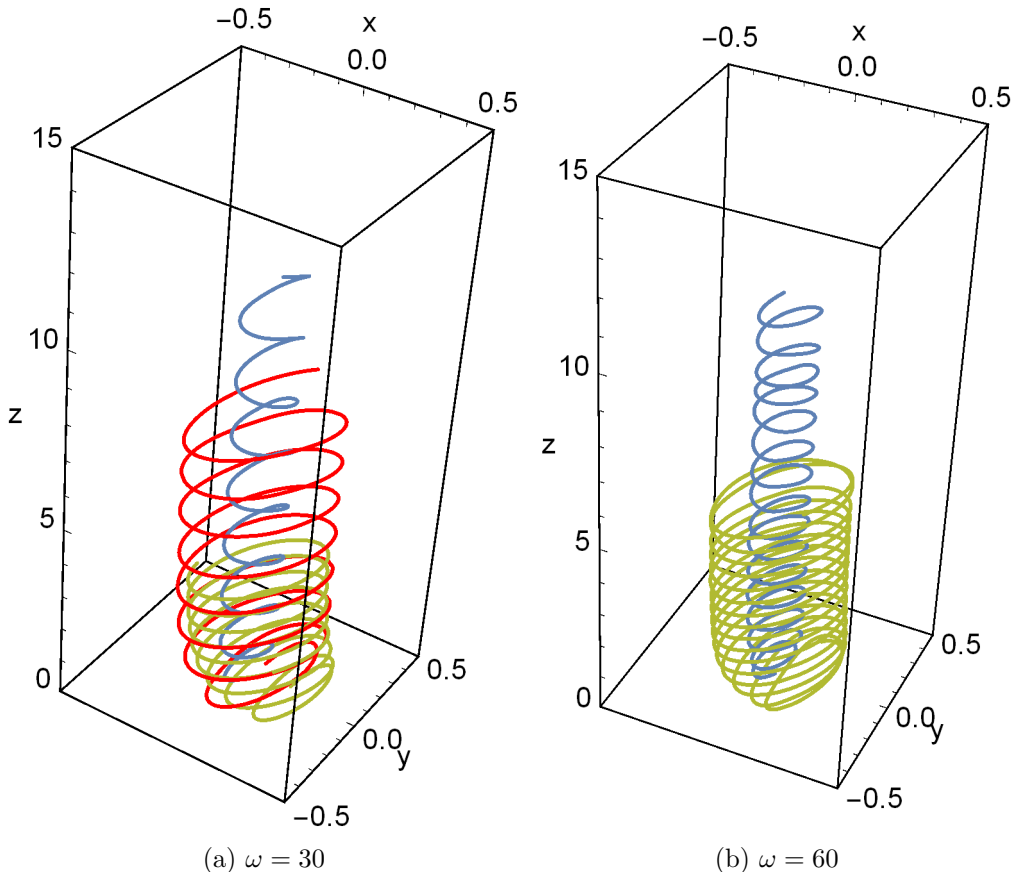

(a) $\omega = 30$ (b) $\omega = 60$

Figure 5: $\alpha = \frac{3\pi}{5}$, $\beta = 0$ for all trajectories. (a) Initial positions: $\boldsymbol{R}(0) = (0.1, \frac{\pi}{3}, 0.1)$ (red), $\boldsymbol{R}(0) = (0.13, \frac{5\pi}{3}, 0.6)$ (blue), $\boldsymbol{R}(0) = (0.2, \frac{\pi}{20}, 0.1)$ (green) (b) Initial positions: $\boldsymbol{R}(0) = (0.25, \frac{\pi}{3}, 0.2)$ (green), $\boldsymbol{R}(0) = (0.13, \frac{5\pi}{3}, 0.6)$ (blue).

6   Arrival time distributions

For our experiment the time of first arrival is given by

$$\tau(\boldsymbol{R}_0) = \inf\{t \,|\, Z(t, \boldsymbol{R}_0) = L, \, \boldsymbol{R}_0 \in \mathrm{supp}(\Psi_0)\}, \tag{62}$$

where $\boldsymbol{R}_0 = \boldsymbol{R}(0)$ and $\Psi_0 = \Psi(\boldsymbol{r}, 0)$ are the initial position and wave function (cf. Eq. (16)) of the particle respectively, while $Z(t, \boldsymbol{R}_0)$ is its $z-$coordinate at time t. The support of the initial wave function Ψ_0 is given by $\{\boldsymbol{r} = (\imath, \phi, z)|\, 0 < z < 1\}$, which is simply the interior of the trap. For a given pair of $\boldsymbol{R}_0$ and Ψ_0, the time of first arrival is uniquely determined in accordance with equation (62). However, in repeated trials of the experiment, it becomes impossible (in practice) to control the initial particle position $\boldsymbol{R}_0$ precisely; although the initial wave function Ψ_0 can be prepared deterministically (see § 9). Due to varying initial conditions the particle

arrives at apparently random times in each run of the experiment, hence it is desirable to consider the arrival time distribution

$$\varrho(\tau) = \text{Prob}\left(\tau < \text{first arrival time} \leq \tau + \mathrm{d}\tau\right). \tag{63}$$

In order to determine ϱ, we recall the so-called *quantum equilibrium hypothesis*, which asserts that the initial particle positions realized in repeated trials of the experiment are drawn from the $\Psi_0^\dagger \Psi_0$−distribution [35]. Under this assumption, the guidance law (cf. Eq. (8)) implies that the particle position at any later time t is distributed according to $\Psi_t^\dagger \Psi_t$. This property is known as *equivariance*.

Now, consider the cumulative distribution function $F(\tau) = \text{Prob}(\text{first arrival time} \leq \tau)$, which is the probability that the first arrival time $\tau(\boldsymbol{R}_0)$ is less than or equal to some fixed τ. The arrival time distribution ϱ is simply the derivative of F, viz.

$$\begin{aligned}
\varrho(\tau) &= \frac{\mathrm{d}}{\mathrm{d}\tau}\text{Prob}\left(\tau(\boldsymbol{R}_0) \leq \tau\right) \\
&= \frac{\mathrm{d}}{\mathrm{d}\tau}\int_{\{\boldsymbol{R}_0 \in \mathbb{R}^3 | \tau(\boldsymbol{R}_0) \leq \tau\}} \mathrm{d}^3\boldsymbol{R}_0 \ \Psi_0^\dagger \Psi_0(\boldsymbol{R}_0) \tag{64} \\
&= \frac{\mathrm{d}}{\mathrm{d}\tau}\int \mathrm{d}^3\boldsymbol{R}_0 \ \theta\left(\tau - \tau(\boldsymbol{R}_0)\right) \Psi_0^\dagger \Psi_0(\boldsymbol{R}_0) \\
&= \int \mathrm{d}^3\boldsymbol{R}_0 \ \frac{\partial}{\partial\tau}\theta\left(\tau - \tau(\boldsymbol{R}_0)\right) \Psi_0^\dagger \Psi_0(\boldsymbol{R}_0) \tag{65} \\
&= \int \mathrm{d}^3\boldsymbol{R}_0 \ \delta\left(\tau - \tau(\boldsymbol{R}_0)\right) \Psi_0^\dagger \Psi_0(\boldsymbol{R}_0), \tag{66}
\end{aligned}$$

where $\delta(x)$ is the Dirac delta function. We have thus arrived at the result

$$\varrho_{\text{Bohm}}(\tau) = \int_{\text{supp}(\Psi_0)} \mathrm{d}^3\boldsymbol{R}_0 \ \delta\left(\tau(\boldsymbol{R}_0) - \tau\right) \Psi_0^\dagger \Psi_0(\boldsymbol{R}_0). \tag{67}$$

Due to the complicated nature of the Bohmian trajectories, $\varrho_{\text{Bohm}}(\tau)$ can not be determined from equation (67) analytically, except in very special circumstances. Therefore, it can only be approximated numerically from a large ensemble of Bohmian trajectories. However, for certain special initial wave functions the Bohmian trajectories cross the arrival surface $z = L$ only once. In these special cases, the first arrival time distribution, or simply the arrival time distribution can be expressed in terms of the probability current density $\boldsymbol{j}$ [38], which satisfies the continuity equation

$$\frac{\partial}{\partial t}\Psi_t^\dagger \Psi_t(\boldsymbol{r}) + \boldsymbol{\nabla}\cdot\boldsymbol{j}(\boldsymbol{r}, t) = 0. \tag{68}$$

The argument goes as follows: Since the particle crosses $z = L$ only once, the probability that the arrival time $\tau(\boldsymbol{R}_0) > \tau$ equals the probability that the particle is located in the region $z < L$ at time τ, which implies,

$$1 - F(\tau) = \int_{z<L} \mathrm{d}^3\boldsymbol{r} \ \Psi_\tau^\dagger \Psi_\tau(\boldsymbol{r}). \tag{69}$$

Note that the r.h.s follows from the property of equivariance discussed above. Differentiating both sides w.r.t τ, and using equation (68), we arrive at

$$\varrho_{\text{Bohm}}(\tau) = -\int_{z<L} \mathrm{d}^3\boldsymbol{r} \ \frac{\partial}{\partial\tau}\Psi_\tau^\dagger \Psi_\tau(\boldsymbol{r}) = \int_{z<L} \mathrm{d}^3\boldsymbol{r} \ \boldsymbol{\nabla}\cdot\boldsymbol{j}(\boldsymbol{r}, \tau) = \int_{z=L} \boldsymbol{j}(\tau)\cdot\mathrm{d}\boldsymbol{\Sigma}, \tag{70}$$

where $d\boldsymbol{\Sigma}$ is a differential area element pointing along $\hat{\boldsymbol{z}}$. The last step follows from an application of the Gauss divergence theorem. The surface integral of $\boldsymbol{j}$ is called the *quantum flux*, hence we define

$$\varrho_{\mathsf{qf}}(\tau) := \int_{z=L} \boldsymbol{j}(\tau) \cdot d\boldsymbol{\Sigma}. \tag{71}$$

Since $\varrho_{\mathsf{qf}}(\tau)$ is a probability density, it must be non-negative, while the probability current density $\boldsymbol{j}$ can become negative. A negative $\boldsymbol{j}$ implies that the Bohmian trajectories are re-entrant (i.e. they cross $z = L$ more than once), in which case equation (69) becomes invalid. This caveat is almost always overlooked in the literature, and the Bohmian arrival time is said to be given by the quantum flux ϱ_{qf} in all circumstances. In general, there is no known simple formula (like Eq. (71)) for the first arrival time distribution of a particle. As an illustration, we will later show that $\varrho_{\mathsf{Bohm}} \neq \varrho_{\mathsf{qf}}$ for the up-down wave function.

The quantum flux can be explicitly written as

$$\varrho_{\mathsf{qf}}(\tau) = \int_0^{2\pi} d\phi \int_0^\infty d\imath \, \imath \, j_z(\imath, \phi, L, \tau), \tag{72}$$

where j_z is the $z-$component of $\boldsymbol{j}$, which for a spin-1/2 particle takes the form [36, 37]

$$\boldsymbol{j}(\boldsymbol{r}, t) = \mathrm{Im}\big[\Psi^\dagger \boldsymbol{\nabla} \Psi\big](\boldsymbol{r}, t) + \frac{1}{2}\boldsymbol{\nabla} \times (\Psi^\dagger \boldsymbol{\sigma} \Psi)(\boldsymbol{r}, t). \tag{73}$$

This gives for the $z-$component of the current density

$$j_z(\boldsymbol{r}, t) = \frac{2\omega}{\pi} \exp(-\omega \imath^2)\Big(\mathrm{Im}[W^* W'](z, t) + \omega \imath \, \sin \alpha \, \sin(\phi - \beta) \, |W|^2(z, t)\Big). \tag{74}$$

Plugging this expression into equation (72), we obtain

$$\varrho_{\mathsf{qf}}(\tau) = 2 \, \mathrm{Im}[W^* W'](L, \tau). \tag{75}$$

Note that ϱ_{qf} is independent of the trapping frequency ω, and the spin orientation angles α and β. See Fig. 6 for plots of ϱ_{qf} for select values of L. The distribution has a large main lobe preceded by infinitely many smaller lobes. The zeros of $\varrho_{\mathsf{qf}}(\tau)$ are given by $\frac{L}{n\pi}$, $n = 2, 3, 4 \dots$ approximately. With increasing L, the main lobe becomes positively skewed (or skewed to the left).

The natural question that arises at this point is, which initial ground state wave functions (if any) give ϱ_{qf} for the first arrival time distribution? In order to answer this question, consider the $z-$component of the Bohmian velocity field (cf. Eq. (43) and (49)) evaluated on the arrival surface $z = L$, viz.

$$v_z(\boldsymbol{r}, t)|_{z=L} = \mathrm{Im}\Big[\frac{W'}{W}\Big](L, t) + \omega \imath \, \sin \alpha \, \sin(\phi - \beta), \tag{76}$$

whose sign determines the direction of crossing of the Bohmian trajectory passing through the point $(\imath, \phi, L)$ at time t. It turns out that the first term, viz. $\mathrm{Im}[W'/W](L, t)$ is non-negative for $t > 0$ and $L > 1$, while the second term becomes negative whenever $\sin(\phi - \beta) < 0$.[7] Therefore,

$$v_z(\boldsymbol{r}, t)|_{z=L} \geq 0, \qquad \forall \, t > 0 \tag{77}$$
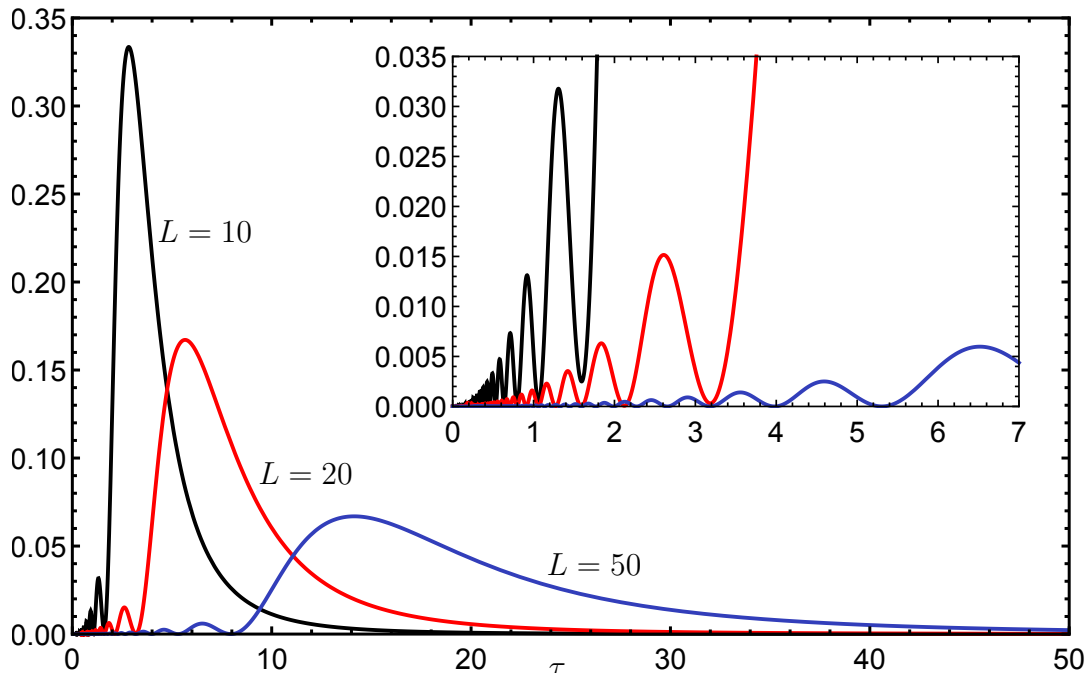
---

[7]Since $0 \leq \alpha \leq \pi$, $\sin \alpha \geq 0$.

Figure 6: Graphs of $\varrho_{\mathsf{qf}}(\tau) = 2\,\mathrm{Im}[W^*W'](L,\tau)$ for select values of L. The zeros of the distribution occur at $\approx \frac{L}{n\pi}$, $n = 2, 3, 4 \ldots$

if $\alpha = 0$ or $\alpha = \pi$, which correspond to the spin-up and spin-down wave functions respectively. Hence, the spin-up and spin-down Bohmian trajectories cross the arrival surface only once, consequently the arrival time distribution in these cases is given by the quantum flux. However, for other spin orientations, (77) may still hold (for instance if ω is small), in which case the distribution of arrival times will be given by the quantum flux.

As remarked earlier, for a general spin orientation we can at best approximate $\varrho_{\mathsf{Bohm}}(\tau)$ from numerical simulations. The strategy for achieving this, given a particular α is quite simple:

1. Sample N initial positions from the

$$\Psi_0^\dagger \Psi_0 = \frac{2\omega}{\pi} \theta(z)\theta(1-z)\sin^2(\pi z)\exp(-\omega z^2) \tag{78}$$

   distribution. This is called the quantum equilibrium ensemble.

2. Solve the equations of motion (cf. Eq. (52)) numerically for each initial position in the ensemble, until the trajectory hits the arrival surface $z = L$.

3. Record the instant of arrival for the N simulations and plot the (area normalized) histogram of arrival times.

For N large, the obtained histogram approximates $\varrho_{\mathsf{Bohm}}(\tau)$.

7   Results and discussion

For generating the quantum equilibrium ensemble we use the *inverse transform sampling* method, while the equations of motion have been integrated with Wolfram Mathematica's `NDsolve[]` numerical differential equation solver. With $N \approx 10^4$, we obtain very satisfactory results.

Since we have employed dimensionless variables from the very beginning (cf. Eq. (15)), it is useful to recall that all lengths (such as L) and all times (such as τ) are measured in units of the trap width d and $md^2/\hbar$, respectively. If we take a proton ($m \approx 1.67 \times 10^{-27}\,\text{kg}$) for the spin-1/2 particle and a trap of width $d \approx 10\,\mu\text{m}$, $md^2/\hbar \approx 1.6\,\text{ms}$, hence $L = 10$ would correspond to $0.1\,\text{mm}$ and $\tau = 5$ for instance, would be about $8\,\text{ms}$. Similarly, the trapping frequency ω is measured in units of $\hbar/md^2 \approx 0.63\,\text{kHz}$. Therefore, $\omega = 80$ corresponds to $50.4\,\text{KHz}$ approximately, which is comparable to the trapping frequencies realized in linear Paul traps.

7.1 Dependence on β

The arrival time distribution is independent of β. In order to derive this result, consider

$$\eta(t) = \sin(\Phi(t) - \beta), \tag{79}$$

in terms of which the equations of motion (52) can be written as

$$\dot{R}(t) = \sin\alpha\,\eta(t)\mathrm{Re}\left[\frac{W'}{W}\right](Z(t), t), \tag{80a}$$

$$\frac{\dot{\eta}(t)}{1 - \eta^2(t)} = \frac{\sin\alpha}{R(t)}\mathrm{Re}\left[\frac{W'}{W}\right](Z(t), t) + \frac{\omega\cos\alpha}{\sqrt{1 - \eta^2(t)}}, \tag{80b}$$

$$\dot{Z}(t) = \mathrm{Im}\left[\frac{W'}{W}\right](Z(t), t) + \omega\sin\alpha\,\eta(t)R(t). \tag{80c}$$

The initial coordinates of the particle, viz. $R(0)$, $\Phi(0)$ and $Z(0)$ are independently distributed, since the quantum equilibrium distribution (78) is of the separable form. It is also clear that $\Phi(0)$ is distributed uniformly on the interval $[0, 2\pi)$, which implies that $\eta(0) = \sin(\Phi(0) - \beta)$ is distributed on the interval $(-1, 1)$ with density

$$\varrho(\eta(0)) = \frac{1}{\pi\sqrt{1 - \eta^2(0)}}. \tag{81}$$

Equations (80) and (81) do not depend on β, and are equivalent to the original set of equations (52) with $\Phi(0)$ distributed uniformly on $[0, 2\pi)$. Clearly, the distribution of arrival times (which is same for both) is also independent of β. From here on we will set $\beta = 0$ for brevity.

7.2 Dependence on α and ω

The arrival time distributions for spin orientation angles α_1 and α_2, satisfying $\alpha_1 + \alpha_2 = \pi$ are the same. We have already seen a special instance of this result, viz. $\alpha_1 = 0$ (spin-up) and $\alpha_2 = \pi$ (spin-down), where the arrival time distribution was given by the quantum flux. In order to prove this claim, consider $\alpha_1 = \alpha$ and $\alpha_2 = \pi - \alpha$. When plugged into the equations of motion (52), we obtain

$$\dot{\Phi}(t) = \frac{\sin\alpha}{R(t)}\cos\Phi(t)\,\mathrm{Re}\left[\frac{W'}{W}\right](Z(t), t) + \omega\cos\alpha, \tag{82a}$$

$$\dot{\Phi}(t) = \frac{\sin\alpha}{R(t)}\cos\Phi(t)\,\mathrm{Re}\left[\frac{W'}{W}\right](Z(t), t) - \omega\cos\alpha, \tag{82b}$$

respectively for equation (52b), while equations (52a) and (52c) are identical in either case. However, letting $\Phi(t) \rightarrow \pi - \Phi(t)$ in the equations of motion for α_2, makes them exactly identical to those for α_1. Since the initial ϕ−coordinate is distributed uniformly on $[0, 2\pi)$, $\Phi(0)$ and $\pi - \Phi(0)$ are sampled *equally likely*, as a result the ensemble of Bohmian trajectories for α_1 and α_2 are the same, which implies that the arrival time distributions for these spin orientations are also equal. In view of this result, we may only consider $0 \leq \alpha \leq \frac{\pi}{2}$. In Fig. 7 we plot the
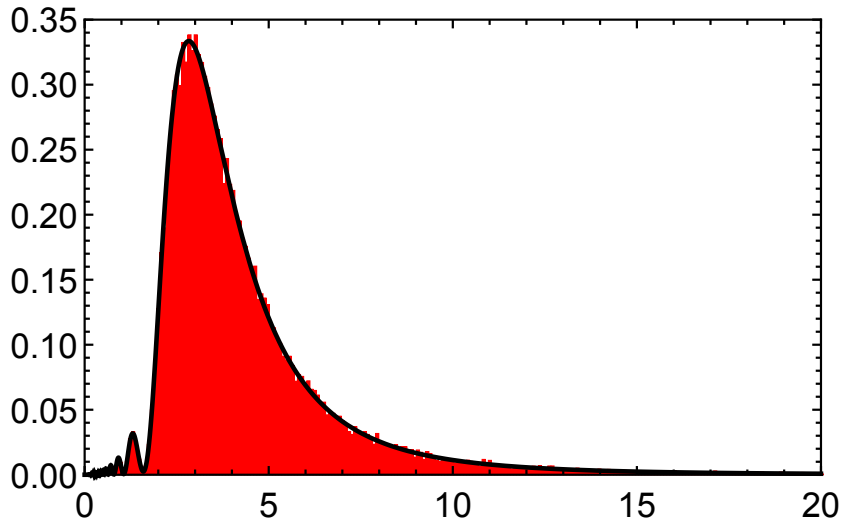

Figure 7: Histogram of arrival times for spin-up wave function (red) for $L = 10$, $\omega = 50$, generated from 8×10^4 Bohmian trajectories. The agreement with $\varrho_{\mathrm{qf}}(\tau)$ (black curve) is clearly seen.

arrival time histogram for the spin-up wave function, which fits the quantum flux very well. At this point one might wonder: which initial positions end up in the main lobe? which initial positions end up in the smaller lobes? We answer these questions with the help of Fig. 8, which shows that particles starting closer to the barrier ($z = 1$) arrive faster compared to those starting at the bottom of the waveguide.

Since the quantum flux is independent of the trapping frequency ω, the arrival time distribution for the spin-up (or spin-down) wave function doesn't change with varying ω. In fact, it turns out that this distribution is also independent of the particular shape of the radial confining potential $V_\perp(z)$, so long as it supports a bound state.

Next, considering the up-down wave function ($\alpha = \frac{\pi}{2}$) we find that the Bohmain arrival time distribution (shown in Fig. 9) is manifestly different from the quantum flux: There seems to be a maximum arrival time τ_{max} beyond which no particles arrive. For arrivals at $L = 10$ we obtain $\tau_{\mathrm{max}} \approx 5.85$ and $\tau_{\mathrm{max}} \approx 4.44$ for trapping frequencies $\omega = 50$ and $\omega = 500$ respectively. We have graphed the mean first arrival time $<\tau>$ as a function of the spin orientation α in Fig. 10.

7.3 Dependence on L

For large L the maxima of the main lobe moves rightwards, as the particles take longer to arrive at the detection surface. However, the surprising results we found previously for the up-down wave function persist. In Fig. 11 we graph the arrival time histogram for this wave function with $L = 10^2$ and $\omega = 10^3$. As before, no particles arrive beyond a characteristic maximum arrival time $\tau_{\mathrm{max}} \approx 42.55$.
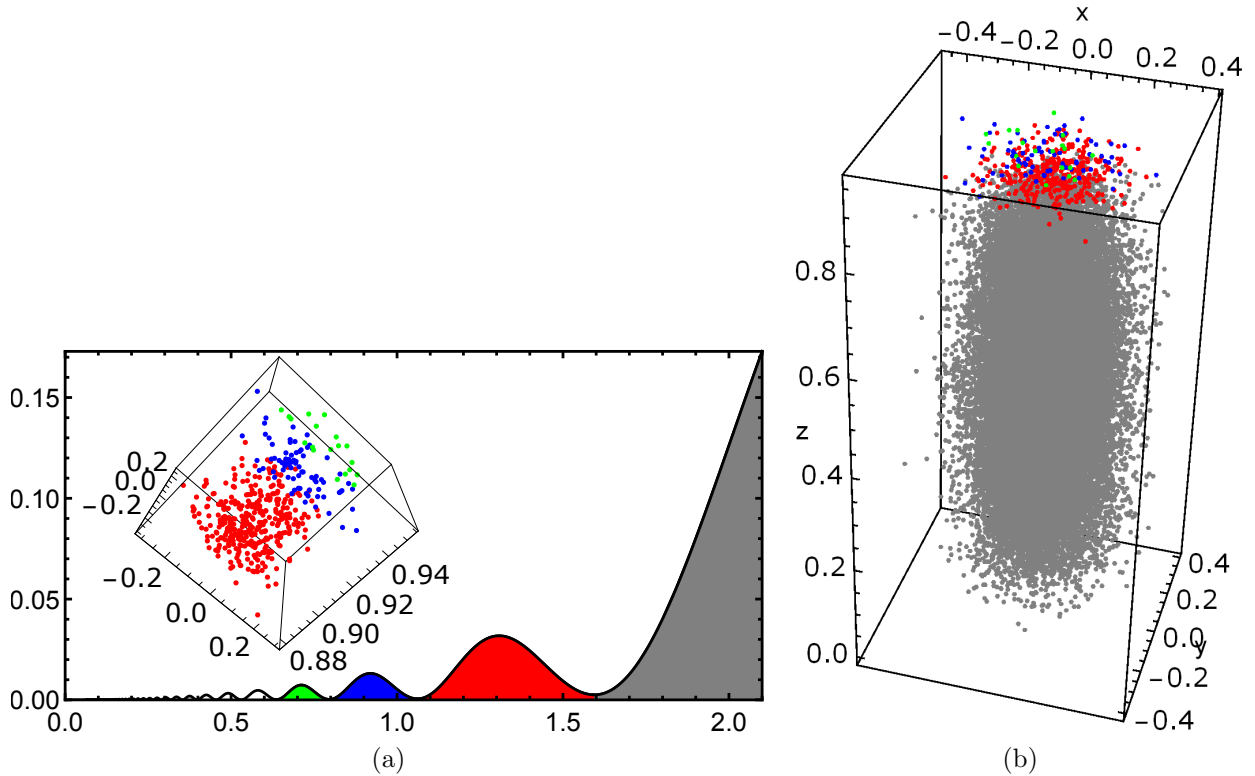
Figure 8: (a) Lobes of $\varrho_{\mathtt{qf}}(\tau)$. Inset: initial particle positions in the vicinity of the barrier. (b) Initial positions sampled from the quantum equilibrium distribution (cf. Eq. (78)). The color code identifies the initial positions with the lobes, they correspond to.
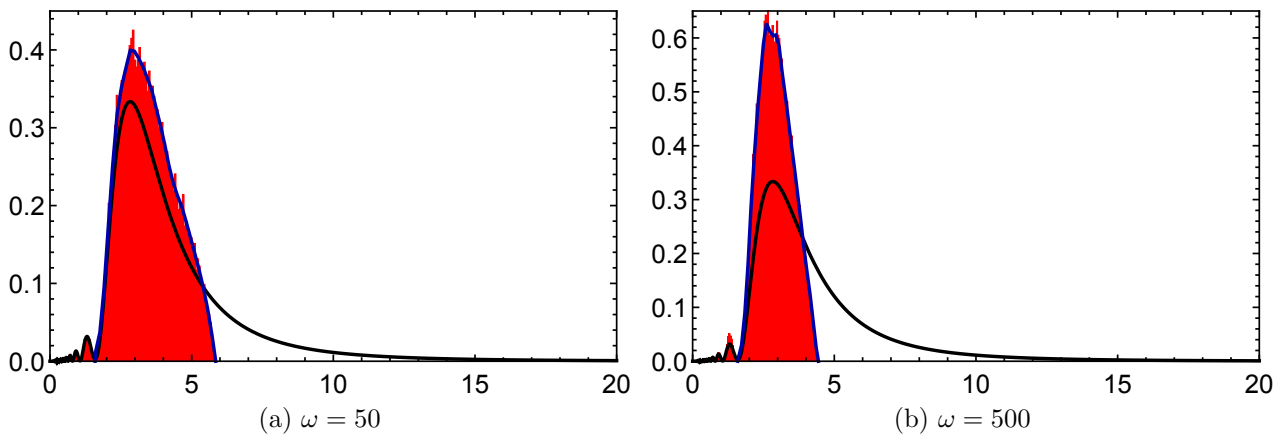

Figure 9: Histogram of arrival times for up-down wave function (red) for $L = 10$, generated from 4×10^4 Bohmian trajectories. The disagreement with $\varrho_{\mathtt{qf}}(\tau)$ (black curve) is clearly seen.

8   Limits of semiclassical analysis

Since the standard interpretation of quantum mechanics fails to account for the time of arrival of particles in a satisfactory manner, semiclassical methods are often employed for interpreting time-of-flight measurements. These measurements are usually performed in the far field (i.e. $L \gg 1$) and the time of arrival statistics is interpreted as a momentum measurement. Such a treatment is usually justified on the grounds that the initial distance from the detector
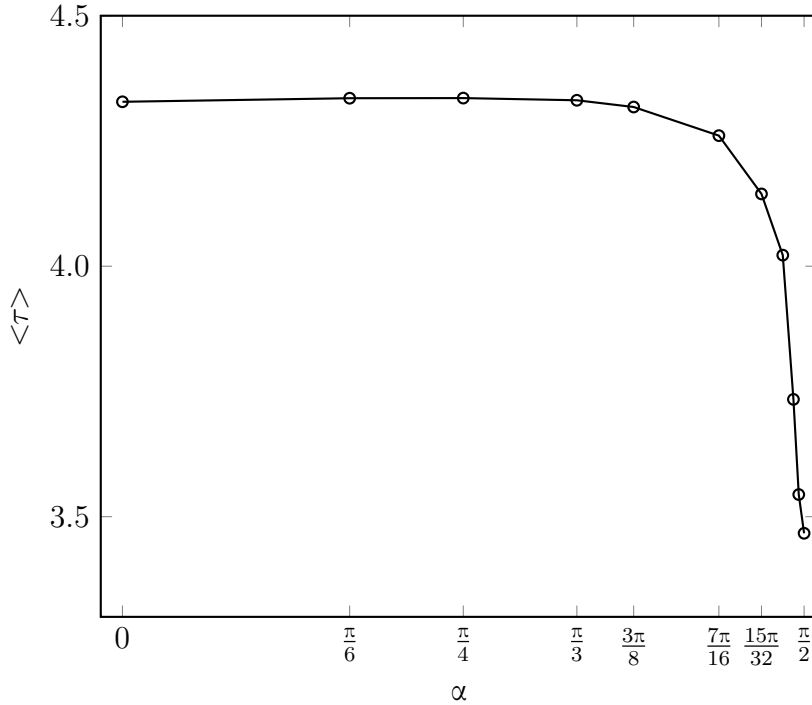
Figure 10: Mean first arrival time $<\tau>$ vs. spin orientation angle α for $L = 10$ and $\omega = 50$.
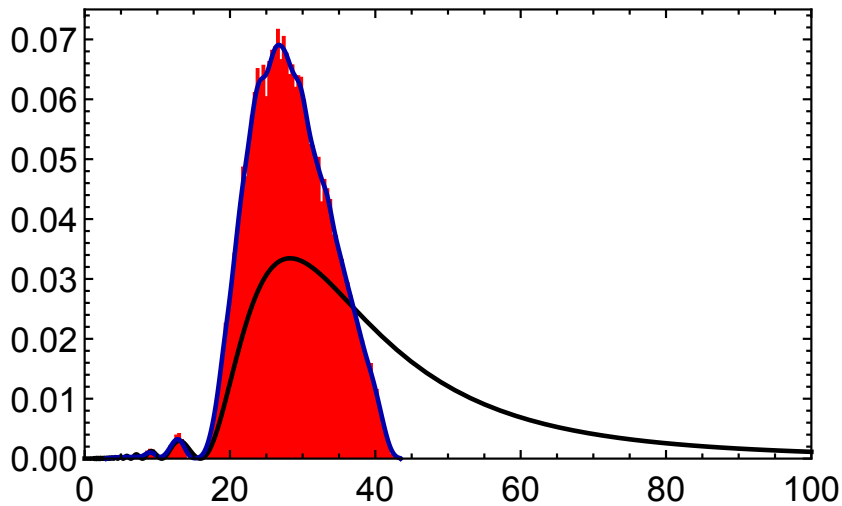

Figure 11: Histogram of arrival times for up-down wave function (red) for $L = 10^2$ and $\omega = 10^3$, generated from 4×10^4 Bohmian trajectories. The disagreement with $\varrho_{\mathtt{qf}}(\tau)$ (black curve) is clearly seen as before.

being much larger than the uncertainty in the initial position of the particle, each particle approximately travels the same length L. Hence, the randomness in the time of arrival is approximately determined by the quantum mechanical momentum distribution. For a free particle in one dimension, the connection between time and momentum is given by $p(t) = mL/t$. By a change of variable, this relation implies that the probability density of the arrival time τ is

$$\varrho_{\mathtt{sc}}(\tau) = \frac{mL}{\hbar \tau^2} \, |\tilde{\psi}|^2 \left(\frac{mL}{\hbar \tau} \right), \tag{83}$$

24

where $\tilde{\psi}$ is the Fourier transform of the wave function ψ. Applying this idea to our experiment, we will show that ϱ_{sc} differs from the Bohmian predictions, even when $L \gg d$.

In order to find the correct generalization of equation (83) for our experiment, consider an ensemble of classical particles subject to the waveguide potential $V(\boldsymbol{r})$ (cf. Eq. (12)), which are subject to Newton's second law of motion (with $\hbar = m = d = 1$)

$$\ddot{\boldsymbol{R}}(t) = -\boldsymbol{\nabla} V(\boldsymbol{r}). \tag{84}$$

Here, $\boldsymbol{R}(t) = R(t)\left[\cos\Phi(t)\,\hat{\boldsymbol{x}} + \sin\Phi(t)\,\hat{\boldsymbol{y}}\right] + Z(t)\,\hat{\boldsymbol{z}}$ denotes the position of the particle at time t. Equation (84) gives three component equations, viz.

$$\ddot{R} - R\dot{\Phi}^2 = -V'_\perp(R), \qquad R\ddot{\Phi} + 2\dot{R}\dot{\Phi} = 0, \qquad \ddot{Z} = -V'_\parallel(Z). \tag{85}$$

The exact solutions of these equations are not needed for our derivation. Note that the first two equations have no bearing on the time of arrival at $z = L$. However, the hard wall placed at $z = 0$ leads to an 'instantaneous reversal' of the sign of $\dot{Z}$, whenever $Z(t) = 0$, i.e. the particle gets reflected elastically on colliding with the wall, and moves with constant velocity subsequently. Denoting the initial $z-$coordinate of the particle by $Z(0)$, the (classical) time of arrival τ is given by

$$\tau = \begin{cases} \dfrac{L - Z(0)}{\dot{Z}(0)} & \dot{Z}(0) > 0 \\[3mm] \dfrac{L + Z(0)}{-\dot{Z}(0)} & \dot{Z}(0) < 0 \end{cases} \quad \text{or} \quad \tau = \frac{L - \mathrm{sgn}[\dot{Z}(0)]\, Z(0)}{|\dot{Z}(0)|}. \tag{86}$$

Since the particle is trapped in the beginning, $0 < Z(0) < 1$. Therefore, if $L \gg 1$, we have

$$\tau(p_z) \approx \frac{L}{|p_z|}, \quad p_z = \dot{Z}(0). \tag{87}$$

This equation implicitly defines the relation between the $z-$component of the initial momentum and the arrival time of a classical particle moving in the potential field $V(\boldsymbol{r})$.

At this stage, one *assumes* that the distribution of momenta of the classical ensemble is determined by the initial wave function of the quantum particle. In particular, the momenta are distributed according to the density $\tilde{\Psi}_0^\dagger \tilde{\Psi}_0(\boldsymbol{p})$, where

$$\tilde{\Psi}_0(\boldsymbol{p}) = (2\pi)^{-3/2} \int_{\mathbb{R}^3} \mathrm{d}^3\boldsymbol{r}\ \Psi_0(\boldsymbol{r})\, e^{-i\boldsymbol{p}\cdot\boldsymbol{r}} \tag{88}$$

is the Fourier transform of the initial wave function $\Psi_0(\boldsymbol{r})$.

Since the arrival time τ is a function only of the $z-$momenta p_z we can integrate out (marginalize) p_x and p_y, obtaining

$$\Lambda(p_z) = \int_{-\infty}^\infty \mathrm{d}p_x \int_{-\infty}^\infty \mathrm{d}p_y\ \tilde{\Psi}_0^\dagger \tilde{\Psi}_0(\boldsymbol{p}). \tag{89}$$

Now, we will obtain a formula for the distribution of first arrival times of the ensemble in terms of Λ. To achieve this, consider the cumulative distribution function $F(\tau) = \mathrm{Prob}(\tau(p_z) \le \tau)$, which is the probability that the arrival time $\tau(p_z)$ is less than or equal to some fixed τ. Using equation (87), we can write

$$F(\tau) = \mathrm{Prob}\left(\frac{L}{|p_z|} \le \tau\right) = \mathrm{Prob}\left(|p_z| \ge \frac{L}{\tau}\right)$$
$$= \int_{-\infty}^{-L/\tau} \mathrm{d}p_z\ \Lambda(p_z) + \int_{L/\tau}^\infty \mathrm{d}p_z\ \Lambda(p_z). \tag{90}$$

The distribution of first arrival times $\varrho_{\mathrm{sc}}(\tau)$ is simply the derivative of F w.r.t τ, which is given by

$$\varrho_{\mathrm{sc}}(\tau) = \frac{L}{\tau^2}\left(\Lambda\left(\frac{L}{\tau}\right) + \Lambda\left(-\frac{L}{\tau}\right)\right). \tag{91}$$

Using the closed expression for the marginal momentum density obtained in appendix C, we are led to

$$\varrho_{\mathrm{sc}}(\tau) = \frac{8\pi L}{\tau^2}\frac{\cos^2(L/2\tau)}{((L/\tau)^2 - \pi^2)^2}. \tag{92}$$

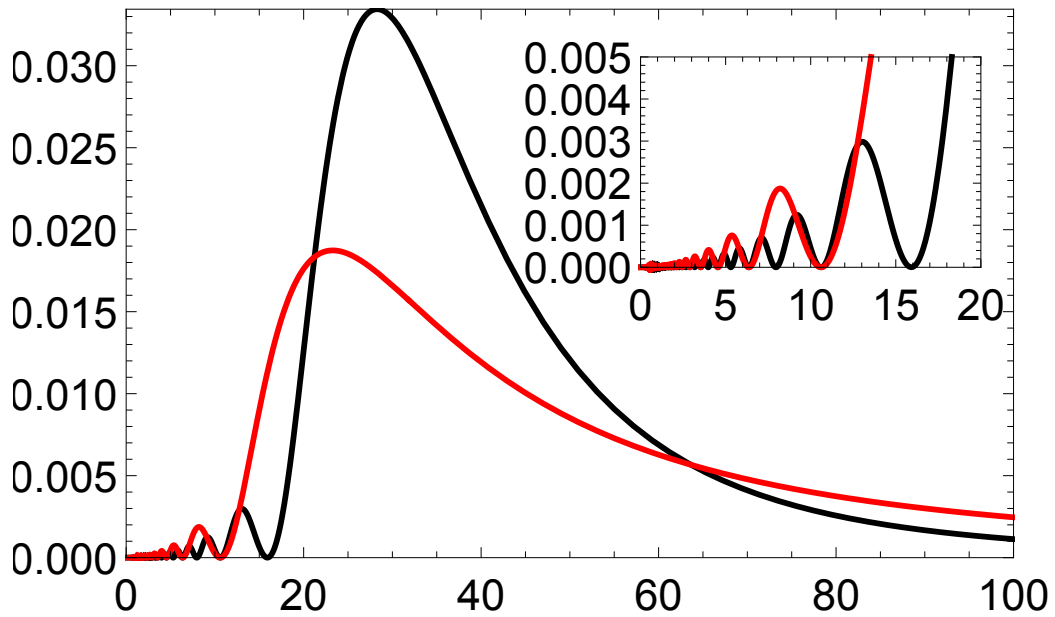This distribution has been graphed along with the quantum flux in the figure below.

Figure 12: Graphs of $\varrho_{\mathrm{sc}}(\tau)$ (red) and $\varrho_{\mathrm{qf}}(\tau)$ (black) for $L = 100$.

9 Experimental Considerations

As remarked in our introduction, the intrinsic (i.e. measurement independent) arrival time distributions discussed here cannot be obtained directly due to the disturbances (or delays) caused by the measuring apparatus. Some authors have addressed this problem by including the detector (a clock for instance) into the Hamiltonian, treating this clock + particle system to be otherwise isolated (see Ch. 8 of [1], [39]). These approaches yield model dependent results, while a physical realization of the clock Hamiltonian is a further concern. Another interesting measurement proposal made by Damborenea et al. [40] seems to be better suited for our experiment.

The proposal of Damborenea et al. is aimed at measuring the arrival time of a two-level atom, which upon entering the detection region (say $z > L$) encounters a cavity impregnated with photons. The time at which the atom emits the first photon, following an absorption is claimed to be a good approximation to the time of arrival of the atom. In order to subtract the various delays (finite absorption and emission times, photon travel times etc.) they consider another (identical) atom at rest placed in the same cavity, which serves as a reference system. Clearly the arrival time of the reference atom is zero, and the first photon emission time of the

same is a measure of the delays caused by our measuring apparatus. On carefully subtracting these delays by means of a deconvolution procedure, they find (for a one dimensional model) that the intrinsic arrival time of the two-level atom equals the quantum flux, under this operational measurement prescription.

In three dimensions however, as we have shown, the intrinsic arrival time distribution (as determined from a Bohmian analysis) can be significantly different from the quantum flux for certain initial wave functions. Therefore, a full three dimensional analysis of Damborenea et al.'s operational proposal becomes necessary. Since we wish to measure the arrival times of a spin-1/2 particle instead of a two-level atom, we have to modify the above proposal appropriately. We suggest that a static magnetic field $\boldsymbol{B}$ be added to the region $z > L$ in addition to the laser field. This would cause the doubly-degenerate ground state of the spin-1/2 particle to split, which would then function as an effective two-level system. A detailed Bohmian analysis of the measurement procedure is hoped to appear in a future paper.

9.1 Initial state preparation

A naive approach to preparing a particle in the ground state of a given potential well would require 1.) setting up the potential field in a desired region of space, 2.) directing the particle from a source to this region, 3.) waiting for radiation damping to bring the particle to the ground state [41]. As an alternative to step 3.) one could also stimulate the ground state transition by external electromagnetic fields.

However, this method is not immediately applicable to our advantage, due to the degeneracy of the ground state of the trap. Therefore, in order to prepare the initial wave function (16):

$$\Psi_0(\boldsymbol{r}) = \sqrt{\frac{2m\omega}{\pi\,\hbar\,d}}\,\theta(z/d)\,\theta(1-z/d)\,\sin(\pi z/d)\exp\left(-\frac{m\omega}{2\hbar}\imath^2\right)\begin{pmatrix}\cos(\alpha/2)\\\sin(\alpha/2)\,e^{i\beta}\end{pmatrix} \tag{93}$$

we add a static magnetic field $\boldsymbol{B} = B_0\,\hat{\boldsymbol{n}}$ to the trap region $0 < z < 1$, where

$$\hat{\boldsymbol{n}} = \sin\alpha\,\cos\beta\,\hat{\boldsymbol{x}} + \sin\alpha\,\sin\beta\,\hat{\boldsymbol{y}} + \cos\alpha\,\hat{\boldsymbol{z}} \tag{94}$$

specifies the direction of the magnetic field. The relevant Hamiltonian is given by [36]

$$\hat{H}_{\texttt{prep}} = \frac{(\boldsymbol{\sigma}\cdot\hat{\boldsymbol{\pi}})^2}{2m} + V_\perp(\imath) + V_\parallel^{\texttt{bar}}(z) = \frac{\hat{\boldsymbol{\pi}}^2}{2m} - \frac{\hbar q}{2m}\,\boldsymbol{\sigma}\cdot\boldsymbol{B} + V_\perp(\imath) + V_\parallel^{\texttt{bar}}(z) \tag{95}$$

where $\hat{\boldsymbol{\pi}} = -i\hbar\boldsymbol{\nabla} - q\boldsymbol{A}$ (in SI units) and $\boldsymbol{A}$ is the electromagnetic vector potential, defined by the equations

$$\boldsymbol{\nabla}\times\boldsymbol{A} = \boldsymbol{B}, \qquad \boldsymbol{\nabla}\cdot\boldsymbol{A} = 0. \tag{96}$$

The axial potential $V_\parallel^{\texttt{bar}}(z)$ is comprised of the impenetrable potential barriers located at $z = 0$ and $z = d$ (cf. Eq. (A.2)). For simplicity, we assume that $\boldsymbol{A}$ varies slowly in the trap region for the dipole approximation $\hat{\boldsymbol{\pi}} \approx -i\hbar\boldsymbol{\nabla} - q\overline{\boldsymbol{A}}$ to be valid. Here, $\overline{\boldsymbol{A}}$ denotes the value of $\boldsymbol{A}$ evaluated at the center of the trap, viz. $(0, 0, d/2)$.[8] Due to the static magnetic field, the degeneracy of the ground state gets lifted. The new ground state wave function is given by

$$\overline{\Psi}_0(\boldsymbol{r}) = \exp\left(\frac{iq}{\hbar}\,\boldsymbol{r}\cdot\overline{\boldsymbol{A}}\right)\Psi_0(\boldsymbol{r}). \tag{97}$$

---

[8]The dipole approximation can be dispensed with in a rigorous analysis of the preparation procedure, without affecting the conclusions.

Thus, a trapped spin-1/2 particle would evolve into the state $\overline{\Psi}_0$ by radiation damping in the presence of the magnetic field. Once in this state (say at time $t = t^*$) the subsequent evolution of the wave function is trivial. Now, in order to recover Ψ_0 from $\overline{\Psi}_0$, one could switch on Lamb's pulsed potential [41]

$$U(t) = q\left(\boldsymbol{r}\cdot\overline{\boldsymbol{A}}\right)\delta(t - t^*) \tag{98}$$

to kill the unwanted phase factor $\exp\left(\frac{iq}{\hbar}\boldsymbol{r}\cdot\overline{\boldsymbol{A}}\right)$ instantaneously, thus obtaining Ψ_0. A more practical alternative for achieving the same would be to switch off the background magnetic field $\boldsymbol{B}$ slowly, after time t^* keeping it's direction $\hat{\boldsymbol{n}}$ undisturbed. The Adiabatic theorem would as a result, ensure that the wave function $\overline{\Psi}_0$ evolves to Ψ_0 at the instant when $\boldsymbol{B} = 0$.

10 Conclusion

In this thesis we discussed the time of arrival statistics of spin-1/2 particles within the framework of Bohmian mechanics. Analyzing a realistic experiment, we obtained several interesting predictions hitherto unknown. It must be emphasized that empirical confirmation of our predictions would not prove the 'reality' Bohmian trajectories, although it would provide strong experimental evidence in their favor. We hope that our results will encourage many experimental investigations in the near future.

A   Ground state wave function

For $t < 0$ the particle is trapped in the region between the planes $z = 0$ and $z = 1$. The relevant Hamiltonian is given by

$$\hat{H}_{\texttt{trap}} = -\frac{1}{2}(\boldsymbol{\sigma}\cdot\boldsymbol{\nabla})^2 + V_\perp(\imath) + V_\parallel^{\texttt{bar}}(z), \tag{A.1}$$

where $V_\perp(\imath) = \frac{1}{2}\omega^2\imath^2$ and

$$V_\parallel^{\texttt{bar}}(z) = \begin{cases} 0 & 0 \le z \le 1 \\ \infty & \text{otherwise} \end{cases}. \tag{A.2}$$

In this appendix we will sketch the derivation of the ground state wave function $\Psi_0(\boldsymbol{r})$, which satisfies the eigenvalue equation

$$\hat{H}_{\texttt{trap}}\Psi_0 = E_0\Psi_0, \tag{A.3}$$

where E_0 is the ground state energy eigenvalue. Note, as a result of identity (19), the Hamiltonian becomes diagonal, hence the desired wave function may be written as

$$\Psi_0(\boldsymbol{r}) = \psi_0(\boldsymbol{r})\chi, \tag{A.4}$$

where $\psi_0(\boldsymbol{r})$ is the spatial wave function and χ is a constant spinor normalized to unity. The spatial wave function thus satisfies the differential equation

$$-\frac{1}{2}\nabla^2\psi_0 + \frac{1}{2}\omega^2\imath^2\psi_0 = E_0\psi_0, \tag{A.5}$$

subject to the usual boundary conditions

$$\psi_0(z = 0) = \psi_0(z = 1) = 0, \quad \lim_{r \to \infty} r\, \psi_0(\boldsymbol{r}) = 0.$$

The continuous, single-valued normalized solutions of equation (A.5), which satisfy the above boundary conditions are well known in the literature (see pp. 727 of [33]). The desired ground state wave function is given by

$$\psi_0(\boldsymbol{r}) = \sqrt{\frac{2\omega}{\pi}}\, \theta(z)\theta(1-z)\sin(\pi z)\exp\left(-\frac{\omega}{2}r^2\right), \tag{A.6}$$

where $\theta(x)$ is the Heavside step function. It corresponds to the energy eigenvalue

$$E_0 = \omega + \frac{\pi^2}{2}. \tag{A.7}$$

Further, writing the unit spinor as

$$\chi = \begin{pmatrix} \cos(\alpha/2) \\ \sin(\alpha/2)\, e^{i\beta} \end{pmatrix}, \tag{A.8}$$

we obtain a convenient representation for the spin part of the ground state wave function. Here, $0 \le \alpha \le \pi$ and $0 \le \beta < 2\pi$ are real parameters.

B Time evolution integral

In this appendix we will obtain a closed expression for the time evolution integral

$$W(z,t) = \theta(z)\int_{-\infty}^{\infty}\mathrm{d}k\ \frac{\sin k \sin(kz)}{\pi^2 - k^2}\, e^{-i\frac{k^2}{2}t}, \tag{B.1}$$

where $t \ge 0$. Letting

$$f(k) = \frac{\sin k \sin(kz)}{\pi^2 - k^2}, \quad g(k) = e^{-i\frac{k^2}{2}t} \tag{B.2}$$

we may view the integral as the inner product of these functions, viz.

$$W(z,t) = \theta(z)\int_{-\infty}^{\infty}\mathrm{d}k\ f^*(k)g(k). \tag{B.3}$$

Using Plancherel's formula we can write

$$W(z,t) = \theta(z)\int_{-\infty}^{\infty}\frac{\mathrm{d}x}{2\pi}\ F^*(x)G(x), \tag{B.4}$$

where F and G are the Fourier transforms of the functions f and g respectively. The Fourier transform of a Gaussian is well known, viz.,

$$G(x) = \int_{-\infty}^{\infty}\mathrm{d}k\ g(k)\, e^{-ikx} = \int_{-\infty}^{\infty}\mathrm{d}k\ e^{-i\frac{k^2}{2}t - ikx} = \sqrt{\frac{2\pi}{it}}\, e^{i\frac{x^2}{2t}}. \tag{B.5}$$

Next, defining

$$y(k) = \frac{1}{\pi^2 - k^2}, \tag{B.6}$$

29

the Fourier transform of $f(k)$ can be written as

$$F(x) = \int_{-\infty}^{\infty} dk\, f(k)\, e^{-ikx} = \int_{-\infty}^{\infty} dk\,\sin k\,\sin(kz)\, y(k)\, e^{-ikx}$$

$$= \frac{1}{4}\int_{-\infty}^{\infty} dk\,\left\{ e^{-i(z-1)k} - e^{-i(z+1)k} - e^{i(z+1)k} + e^{i(z-1)k} \right\} y(k)\, e^{-ikx}$$

$$= \frac{1}{4}\left\{ Y(x+z-1) - Y(x+z+1) - Y(x-z-1) + Y(x-z+1) \right\}, \qquad \text{(B.7)}$$

where $Y(x)$ is the Fourier transform of $y(k)$, given by

$$Y(x) = \int_{-\infty}^{\infty} dk\,\frac{e^{-ikx}}{\pi^2 - k^2} = \frac{1}{2\pi}\int_{-\infty}^{\infty} dk\,\frac{e^{-ikx}}{k+\pi} - \frac{1}{2\pi}\int_{-\infty}^{\infty} dk\,\frac{e^{-ikx}}{k-\pi}$$

$$\text{(letting } u = k \pm \pi\text{)}$$

$$= \frac{e^{i\pi x}}{2\pi}\int_{-\infty}^{\infty} du\,\frac{e^{-ixu}}{u} - \frac{e^{-i\pi x}}{2\pi}\int_{-\infty}^{\infty} du\,\frac{e^{-ixu}}{u}$$

$$= \frac{i}{\pi}\sin(\pi x) \times (-i\pi)\,\mathrm{sgn}(x) = \mathrm{sgn}(x)\sin(\pi x), \qquad \text{(B.8)}$$

and the Fourier transform of u^{-1} is $-i\pi\,\mathrm{sgn}(x)$, in the sense of distributions. Substituting equations (B.5) and (B.7) in equation (B.4), we arrive at

$$W(z,t) = \frac{\theta(z)}{2^{5/2}\sqrt{\pi i t}}\int_{-\infty}^{\infty} dx\,\left\{ Y^*(x+z-1) - Y^*(x+z+1) - Y^*(x-z-1) + Y^*(x-z+1) \right\} e^{i\frac{x^2}{2t}}$$

$$= \frac{\theta(z)}{2^{5/2}\sqrt{\pi i t}}\int_{-\infty}^{\infty} du\, Y^*(u)\left\{ e^{i\frac{(u+1-z)^2}{2t}} - e^{i\frac{(u-1-z)^2}{2t}} - e^{i\frac{(u+1+z)^2}{2t}} + e^{i\frac{(u+z-1)^2}{2t}} \right\}, \qquad \text{(B.9)}$$

after substituting $u = x \pm 1 \pm z$ appropriately in each of the previous terms. Note that the integrand is a symmetric function of u, hence

$$W(z,t) = \frac{\theta(z)}{2^{3/2}\sqrt{\pi i t}}\int_{0}^{\infty} du\, Y^*(u)\left\{ e^{i\frac{(u+1-z)^2}{2t}} - e^{i\frac{(u-1-z)^2}{2t}} - e^{i\frac{(u+1+z)^2}{2t}} + e^{i\frac{(u+z-1)^2}{2t}} \right\}$$

$$= \theta(z)\left[\mathscr{D}(z-1,t) + \mathscr{D}(1-z,t) - \mathscr{D}(1+z,t) - \mathscr{D}(-1-z,t) \right], \qquad \text{(B.10)}$$

where

$$\mathscr{D}(\xi,t) := \frac{1}{2^{3/2}\sqrt{\pi i t}}\int_{0}^{\infty} du\,\sin(\pi u)\, e^{i\frac{(u-\xi)^2}{2t}} = \frac{1}{2^{3/2}\sqrt{\pi t}}\int_{0}^{\infty} du\,\sin\!\left(\pi u\sqrt{i}\right) e^{-\frac{1}{2t}\left(u - \frac{\xi}{\sqrt{i}} \right)^2}. \qquad \text{(B.11)}$$

$$= \frac{e^{-i\frac{\pi^2}{2}t}}{8i}\left\{ e^{i\pi\xi}\,\mathrm{erfc}\!\left[\frac{i^{3/2}}{\sqrt{2}}\left(\frac{\xi}{\sqrt{t}} - \pi\sqrt{t} \right) \right] - e^{-i\pi\xi}\,\mathrm{erfc}\!\left[\frac{i^{3/2}}{\sqrt{2}}\left(\frac{\xi}{\sqrt{t}} + \pi\sqrt{t} \right) \right] \right\}. \qquad \text{(B.12)}$$

Since the integrand is holomorphic, (B.11) is easily verified by a simple deformation of the integration path that changes the integral into a typical Gaussian integral. Finally, equation (B.12) follows from writing the sine as a sum of complex exponentials, and identifying the resulting integrals as representations of the complementary error function, see equation 7.7.6 of [34].

C Fourier transform of Ψ_0

We need only compute the Fourier transform of the spatial part of the initial wave function Ψ_0, viz.

$$\tilde{\psi}(\boldsymbol{p}) := (2\pi)^{-3/2} \int_{\mathbb{R}^3} \mathrm{d}^3\boldsymbol{r} \; \psi(\boldsymbol{r}) \, e^{-i\boldsymbol{p}\cdot\boldsymbol{r}} \tag{C.1}$$

Since we are working in cylindrical coordinates, it will be convenient to parameterize the $xy-$components of $\boldsymbol{p}$ as

$$p_x = p\cos\vartheta, \qquad p_y = p\sin\vartheta. \tag{C.2}$$

This results in

$$\boldsymbol{p}\cdot\boldsymbol{r} = p_x x + p_y y + p_z z = p\varrho\cos\vartheta\cos\phi + p\varrho\sin\vartheta\sin\phi + p_z z$$
$$= p\varrho\cos(\phi - \vartheta) + p_z z. \tag{C.3}$$

Using the explicit representation of the ground state wave function, along with the result obtained above, we can write

$$\tilde{\psi}(\boldsymbol{p}) = 2\sqrt{\omega} \int_0^\infty \mathrm{d}\varrho \; \varrho \, e^{-\frac{\omega}{2}\varrho^2} \int_0^{2\pi} \frac{\mathrm{d}\phi}{2\pi} \; e^{-ip\varrho\cos(\phi-\vartheta)} \int_0^1 \frac{\mathrm{d}z}{2\pi} \; \sin(\pi z) \, e^{-ip_z z}. \tag{C.4}$$

The integral w.r.t z can be readily evaluated, viz.

$$\int_0^1 \frac{\mathrm{d}z}{2\pi} \; \sin(\pi z) \, e^{-ip_z z} = \frac{e^{-i\frac{p_z}{2}}}{\pi^2 - p_z^2} \cos\left(\frac{p_z}{2}\right), \tag{C.5}$$

while substituting $\phi - \vartheta = \pi + \gamma$, renders the integral over ϕ to the form

$$\int_0^{2\pi} \frac{\mathrm{d}\phi}{2\pi} \; e^{-ip\varrho\cos(\phi-\vartheta)} = \int_{-\pi-\vartheta}^{-\pi-\vartheta+2\pi} \frac{\mathrm{d}\gamma}{2\pi} \; e^{ip\varrho\cos\gamma} = J_0(p\varrho), \tag{C.6}$$

see equation (44) of [31]. Thus, we have arrived at

$$\tilde{\psi}(\boldsymbol{p}) = \frac{2\sqrt{\omega}\, e^{-i\frac{p_z}{2}}}{\pi^2 - p_z^2} \cos\left(\frac{p_z}{2}\right) \int_0^\infty \mathrm{d}\varrho \; \varrho \, J_0(p\varrho) \, e^{-\frac{\omega}{2}\varrho^2} = \frac{2\cos(p_z/2)}{\sqrt{\omega}\,(\pi^2 - p_z^2)} \, e^{-\frac{p^2}{2\omega} - i\frac{p_z}{2}} \tag{C.7}$$

This result follows from the 4th identity in § 6.63 of [32]. Now, we will compute the marginal momentum density $\Lambda(p_z)$ defined by equation (89), which can also be written as ($\mathrm{d}p_x\,\mathrm{d}p_y = p\,\mathrm{d}p\,\mathrm{d}\vartheta$)

$$\Lambda(p_z) = \int_0^{2\pi} \mathrm{d}\vartheta \int_0^\infty \mathrm{d}p \; p \, |\tilde{\psi}|^2(\boldsymbol{p}) = \frac{8\pi}{\omega} \frac{\cos^2(p_z/2)}{(p_z^2 - \pi^2)^2} \int_0^\infty \mathrm{d}p \; p \, e^{-\frac{p^2}{\omega}} = 4\pi \frac{\cos^2(p_z/2)}{(p_z^2 - \pi^2)^2} \tag{C.8}$$

References

[1] Muga J. G. et al., *Time in Quantum Mechanics* Vol. 1 (Springer, Berlin Heidelberg 2008), Ch 1.

[2] Leavens C. R., Phys. Rev. A **58**, 840 (1998)

[3] Nelson E., Phys. Rev. **150** 4, 1079 (1966)

[4] Muga J. G. and Leavens C. R., Phys. Rep. **338**, 353-438 (2000), § 8.4.

[5] Dürr D., Goldstein S., Zanghi N., J. Stat. Phys. **166** (1-4), 959–1055 (2004)

[6] Dürr D., Goldstein S. and Zanghi, N. J Stat Phys **134** 1023 (2009)

[7] Holland P. R., *The Quantum theory of Motion* (Cambridge University Press, UK 1993), Ch. 9-10.

[8] Tumulka R., arXiv: 1601.03715 (2016)

[9] Daumer M. et al., Lett. Math. Phys. **38** 1, 103–116 (1996)

[10] Daumer M. et al., J. Stat. Phys. **88** (3-4), 967–977 (1997)

[11] Vona N., Hinrichs G. and Dürr D., PRL. **111** 22, 220404 (2013)

[12] Bohm D. and Hiley B. J., *The Undivided Universe* (Routledge, London, 1993), pp. 222.

[13] Holland P. and Philippidis C., Phy Rev A **67**, 062105 (2003) doi: 10.1103/PhysRevA.67.062105

[14] Berndl K. et al., Commun. Math. Phys. **173**, 647-673 (1995)

[15] Teufel S. and Tumulka R., Commun. Math. Phys. **258**, 349–365 (2005) doi: 10.1007/s00220-005-1302-0

[16] Dewdney C., Holland P. R. and Kyprianidis C., Phys. Lett. A 119 **6** (1986)

[17] Dewdney C. et al., Nature **336**, 536-544 (1988) doi: 10.1038/336536a0

[18] Dewdney C., Holland P. R. and Kyprianidis C., Phys. Lett. A 121 **3**, 105-110 (1987)

[19] Dewdney C. et al., Phys. Lett. A 102 **7**, 291-294 (1984)

[20] Holland P. R., Phys. Rep 169 **5**, 293-327 (1988)

[21] Colijn C. and Vrscay E. R., Phys. Lett. A 300 **4**, 334-340 (2002)

[22] Colijn C. and Vrscay E. R., Found. of Phys. Lett. 16 **4**, 303-323 (2003)

[23] Timko J. A. and Vrscay E. R., Found. of Phys. 39 **9**, 1055-1071 (2009)

[24] Colijn C. and Vrscay E. R., J. Phys. A 36 **16**, 4689 (2003)

[25] Colijn C. and Vrscay E. R., Phys. Lett. A 327 **2**, 113–122 (2004)

[26] Dewdney C., Holland P. R. and Kyprianidis C., J. Phys. A 20 **14**, 4717 (1987)

[27] Oosterkamp T. H. et al., ASSP **38**, 139-152 (1999)

[28] Werth G., J. Phys. G: Nucl. Part. Phys. **20** 1865 (1994)

[29] Neuhauser et al., Phy Rev A **22** 3, 1137-1140 (1980) doi: 10.1103/PhysRevA.22.1137

[30] http://mathworld.wolfram.com/HeavisideStepFunction.html

[31] Cormack A. M., Acta Cryst. **10**, 354-358 (1957)

[32] Gradshteyn I. S. and Ryzhik I. M., *Table of Integrals Series and Products* 4E (Academic Press Inc., London).

[33] Tannoudji C., Diu B. and Laloë F., *Quantum Mechanics* Vol.1 (John Wiley & Sons, France).

[34] `http://dlmf.nist.gov/7.7`

[35] Dürr D., Goldstein S., Zanghi N., J. Stat. Phys. **67** (5-6), 843–907 (1992)

[36] Shikakhwa M. S., Turgut S.,2 and Pak N. K., Am. J. Phys. **79** (11) (2011)

[37] Hodge W. B., Migirditch S. V., and Kerr W. C., Am. J. Phys. **82** (7) (2014)

[38] Leavens C. R., Phys. Lett. A **178** (1-2), 27-32 (1993)

[39] Peres A., Am. J. Phys. **48** 7, 552-557 (1980)

[40] Damborenea J. A. et al., Phy Rev A **66** 5, 052104 (2002) `doi: 10.1103/PhysRevA.66.052104`

[41] Lamb E. W., Phys. Today **22** 4, 23-28 (1969) `doi: 10.1063/1.3035523`